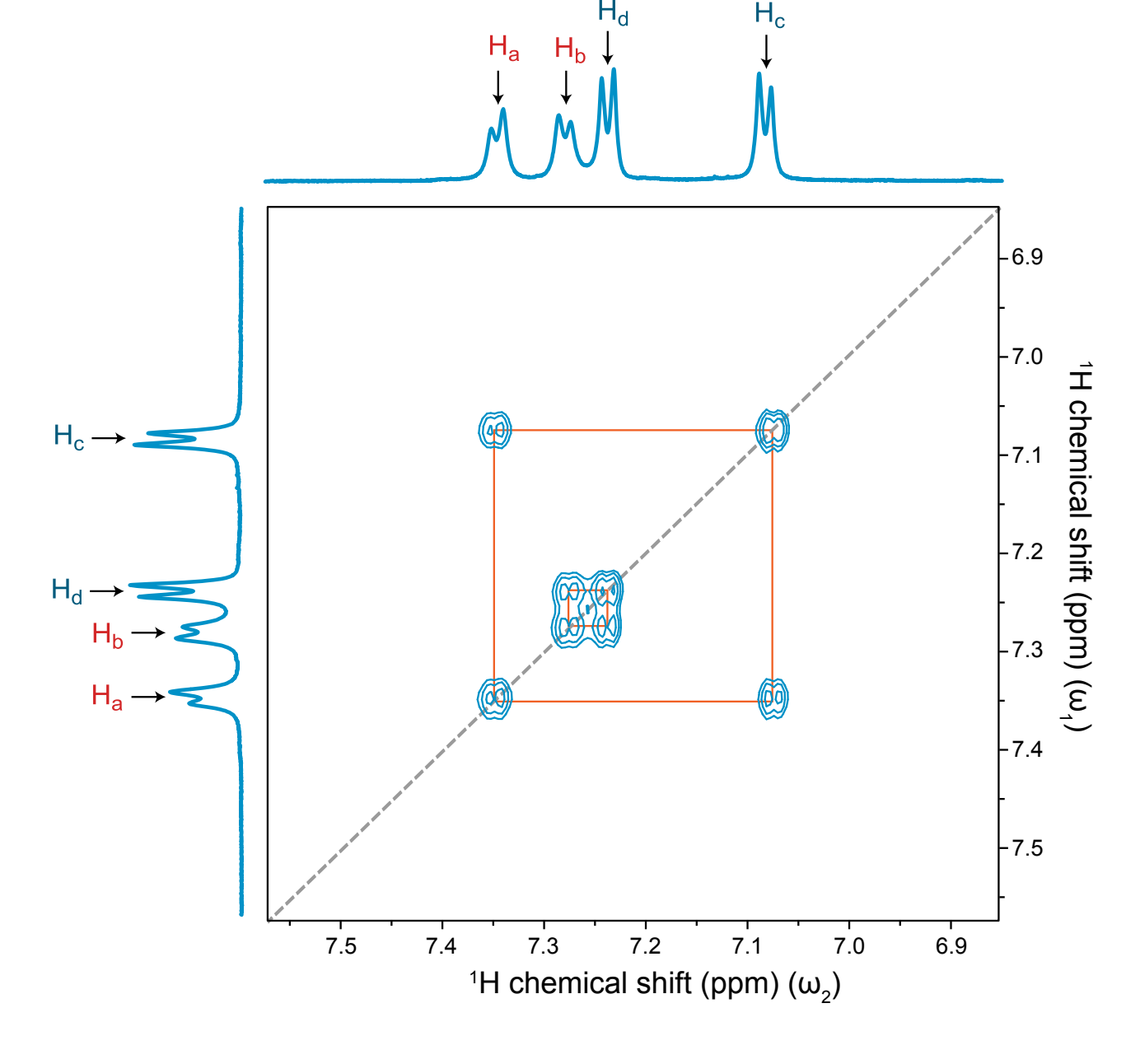


The EXSY experiment yields a correlation between resonances of protons that are exchanging on a timescale comparable to  $\tau_m$ 

Contour plot of the expanded 'aromatic region' of a 2D EXSY <sup>1</sup>H NMR spectrum (700 MHz, D<sub>2</sub>O, pH 6.5) with  $\tau_m$  = 100 ms of a 1:1 mixture of the disulfide and the thiol shown (30 mM total concentration). A 1D spectrum of the mixture is shown on the vertical and horizontal projections.

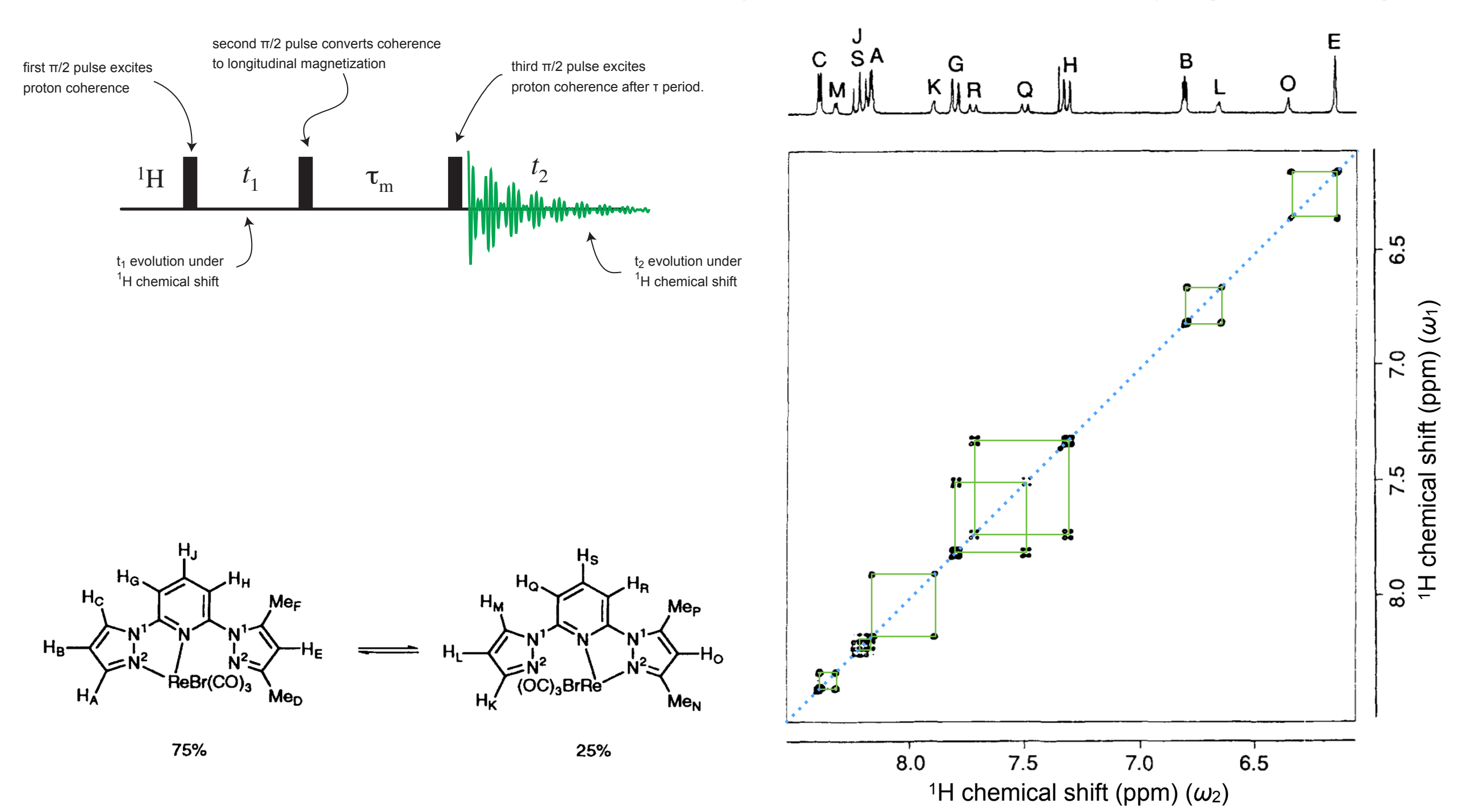
adapted from Bracchi & Fulton, "Orthogonal breaking and forming of dynamic covalent imine and disulfide bonds in aqueous solution." Chem. Commun., **51**, 11052 (2015).



One-dimensional proton NMR spectrum of the organometallic compound [ReBr(CO)3(Me2-bppy)], where bppy denotes 2,6-bis(pyrazol-1-yl)pyridine.

Twice as many peaks as there are types of different protons in the molecule! Must be a second species?

Intensities suggest a 3:1 ratio in concentration between the major and the minor species. Is the second species an impurity, or is it a second product in slow exchange?



Proton two-dimensional exchange spectrum of the organometallic fluxional compound [ReBr(CO)3(Me2-bppy)], where bppy denotes 2,6-bis(pyrazol-1-yl)pyridine. The mixing interval was  $\tau_m = 0.1$  s. The off-diagonal peaks may be interpreted in terms of an exchange of the metal atom between two pairs of nitrogen binding sites.

Adapted from E. W. Abel, et al., J. Chem. Soc. Dalton Trans., 1079 (1994).

# Recall: Modified Bloch Equations

Normally we observe the rate process in the absence of rf fields during free precession periods. Thus, transverse and longitudinal components evolve separately.

$$\frac{d}{dt}\mathbf{M}_{j}^{+} = \left(i\Omega_{j} - \frac{1}{T_{2}}\right)\mathbf{M}_{j}^{+} + \sum_{r} k_{jr}\mathbf{M}_{r}^{+}$$

$$\frac{d}{dt}\mathbf{M}_{jz} = -\frac{1}{T_1} (\mathbf{M}_{jz} - \mathbf{M}_{j0}(t)) + \sum_r k_{jr} \mathbf{M}_{rz}$$

and these equations are conveniently written in matrix form (at equilibrium)

$$\frac{d}{dt}\mathbf{M}^{+} = \mathbf{L}^{+}\mathbf{M}^{+} \tag{3}$$

$$\frac{d}{dt}\mathbf{M}_z = \mathbf{L}\left\{\mathbf{M}_z - \mathbf{M}_0\right\} \tag{4}$$

where  $\mathbf{M}^+$ ,  $\mathbf{M}_z$  and  $\mathbf{M}_0$  contain the magnetization vectors for all J chemical species.

The dynamic matrices L<sup>+</sup> and L describe precession, relaxation, and chemical kinetics

$$\mathbf{L}^+ = i\mathbf{\Omega} - \mathbf{\Lambda} + \mathbf{K}$$

$$L = -R + K$$

 $\Omega$  is a diagonal matrix containing the chemical shifts  $\Omega_i$ .

 $\Lambda$  is also a diagonal matrix of transverse relaxation times  $T_{2i}^{-1}$ .

**R** is the longitudinal relaxation matrix (and for the moment is diagonal containing  $T_{1i}^{-1}$ .

# Longitudinal Exchange in EXSY

EXSY can be used to follow relatively complex reactions, and one may think it difficult to obtain quantative information on the rates, but he dynamics of the longitudinal magnetization during  $\tau_m$  are controlled by equation (4).

$$\frac{d}{dt}\mathbf{M}_z = \mathbf{L}\left\{\mathbf{M}_z - \mathbf{M}_0\right\} \tag{4}$$

which under conditions of dynamic chemical equilibrium (i.e. a stationary state) can be simplified to (net exchange of  $M_0$  is zero)

$$\frac{d}{dt}\Delta\mathbf{M} = \mathbf{L}\Delta\mathbf{M}.$$

This has a formal solution

$$M_z(\tau_m) = M_0 + \exp\{\mathbf{L}\tau_m\}\Delta M_z(\tau_m = 0).$$

Which implies that the magnetization components recover during  $\tau_m$  towards equilibrium. We find that the signal during  $t_2$  is then given by

$$M^+(t_1,\tau_m,t_2) = -\exp\{\mathbf{L}^+t_2\}\exp\{\mathbf{L}\tau_m\}\exp\{\mathbf{L}^+t_1\}M_0.$$

# Longitudinal Exchange in EXSY

$$M^{+}(t_{1},\tau_{m},t_{2}) = -\exp\{\mathbf{L}^{+}t_{2}\}\exp\{\mathbf{L}\tau_{m}\}\exp\{\mathbf{L}^{+}t_{1}\}M_{0}.$$

For slow exchange, lineshapes in  $t_1$  and  $t_2$  are not affected by contributions of **K** to  $\mathbf{L}^+$  and they may be neglected. As a result the time-domain signal simplifies to

 $\omega_1$ 

 $\omega_2$ 

$$s(t_1, \tau_m, t_2) = -\sum_{k} \sum_{l} \exp\{-i\Omega_k t_2 - \lambda_k t_2\} \left[ \exp\{\mathbf{L}\tau_m\} \right]_{k,l} \exp\{-i\Omega_l t_1 - \lambda_l t_1\} M_{l0}.$$

and a fter 2D FT the integrated amplitude of a signal with frequency coordinates  $(\omega_1, \omega_2) = (\Omega_l, \Omega_k)$  is

$$I_{kl}(\tau_m) = a_{kl}(\tau_m) M_{l0}$$
 and  $a_{kl}(\tau_m) = \left[\exp\{\mathbf{L}\tau_m\}\right]_{kl}$ .

The 2D spectrum amounts to a pictorial representation of the exponential mixing operator.

# Longitudinal Exchange in EXSY

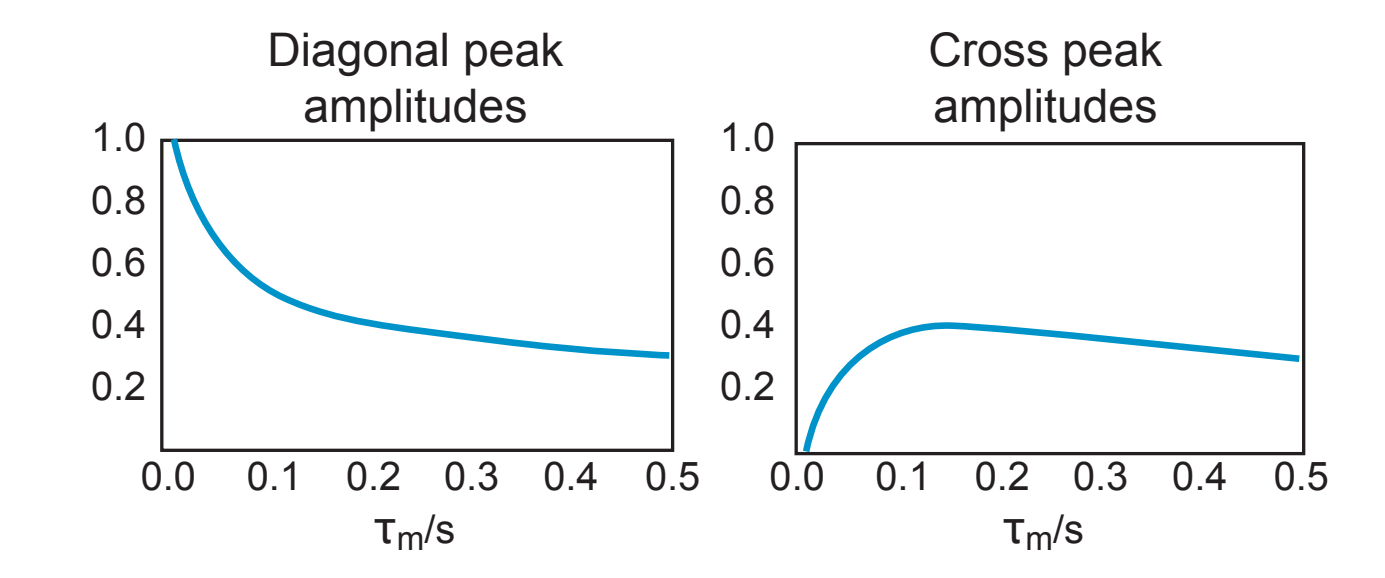
For a 2 spin system, the 2x2 dynamic matrix leads to an analytical solution, and for a symmetrical case we obtain:

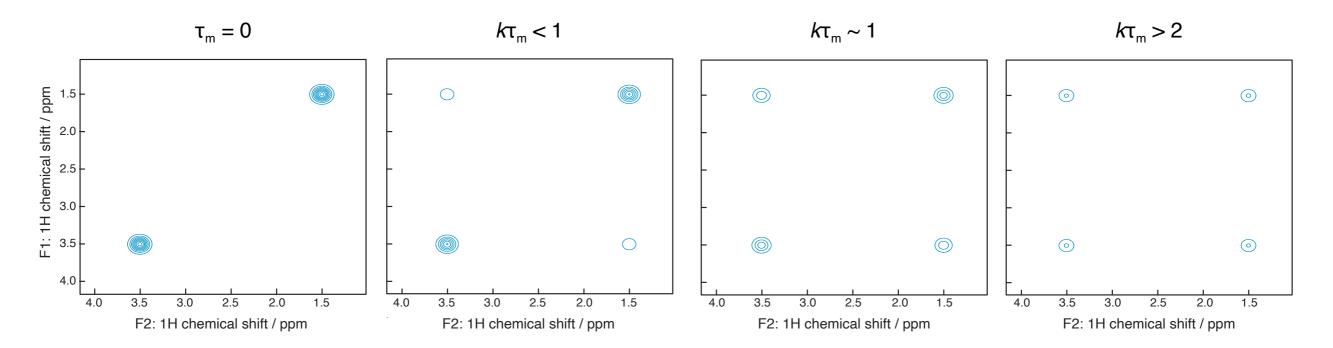
$$I_{AA}(\tau_{m}) = \frac{1}{2} [1 + \exp\{-2k\tau_{m}\}] \exp\{-\tau_{m}/T_{1}\} M_{A0}$$

$$I_{BB}(\tau_{m}) = \frac{1}{2} [1 + \exp\{-2k\tau_{m}\}] \exp\{-\tau_{m}/T_{1}\} M_{B0}$$

$$I_{AB}(\tau_{m}) = \frac{1}{2} [1 - \exp\{-2k\tau_{m}\}] \exp\{-\tau_{m}/T_{1}\} M_{B0}$$

$$I_{BA}(\tau_{m}) = \frac{1}{2} [1 - \exp\{-2k\tau_{m}\}] \exp\{-\tau_{m}/T_{1}\} M_{A0}$$





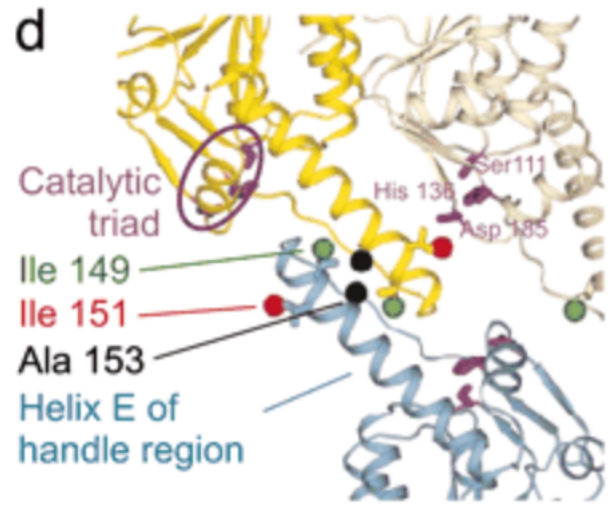


# Quantitative NMR spectroscopy of supramolecular complexes: Dynamic side pores in ClpP are important for product release

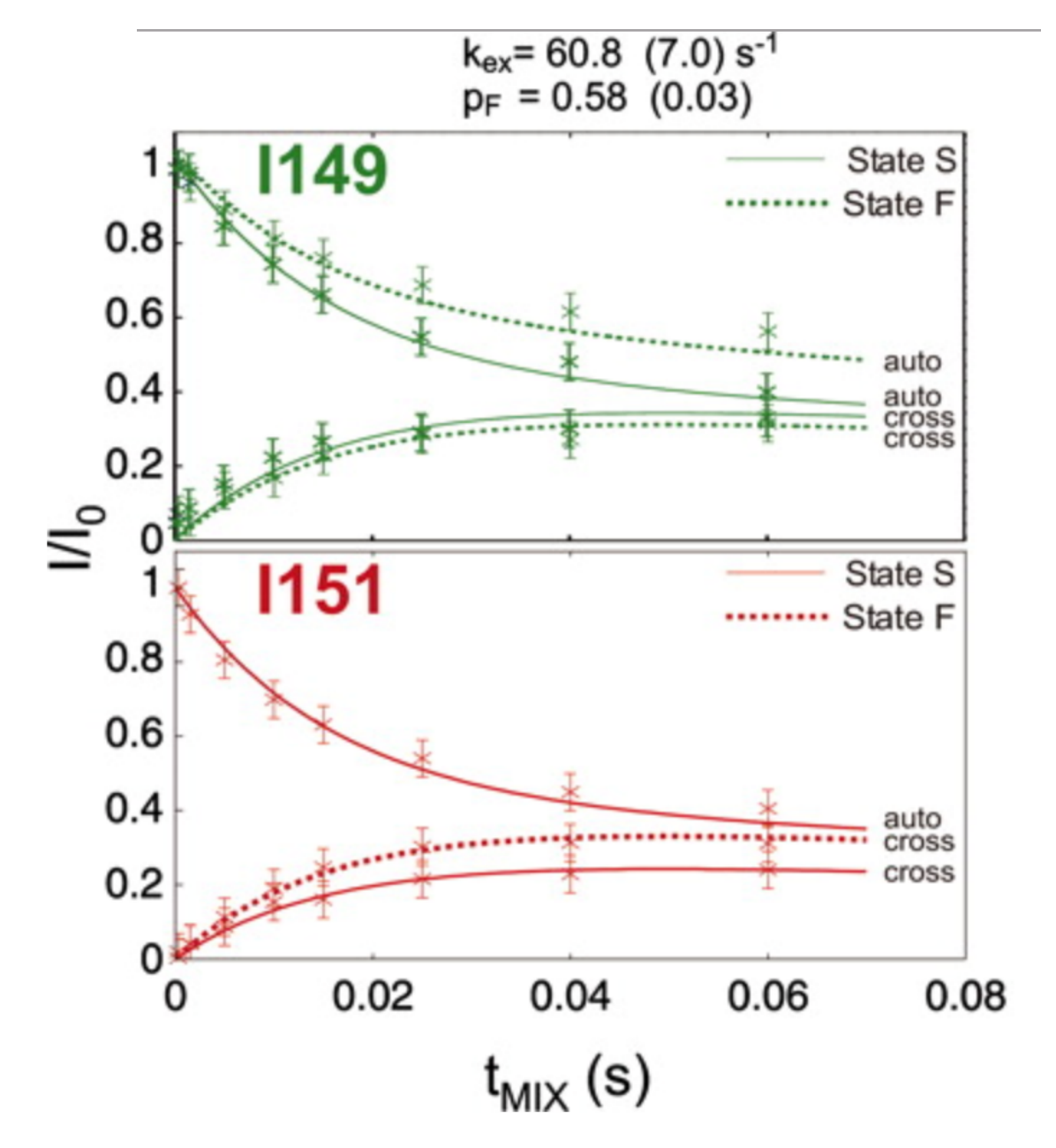
Remco Sprangers\*<sup>†§</sup>, Anna Gribun\*, Peter M. Hwang\*, Walid A. Houry\*<sup>¶</sup>, and Lewis E. Kay\*<sup>†§¶</sup>

Departments of \*Biochemistry, †Medical Genetics, and §Chemistry, University of Toronto, Toronto, ON, Canada M5S 1A8

Edited by Alfred G. Redfield, Brandeis University, Waltham, MA, and approved September 30, 2005 (received for review August 23, 2005)



Abridged Abstract: The 300-kDa cylindrical protease ClpP is an important component of the cellular protein quality machinery. It consists of 14 subunits arranged into two heptameric rings that enclose a large chamber containing the protease active sites. ClpP associates with ClpX and ClpA ATPases that unfold and translocate substrates into the protease catalytic chamber through axial pores located at both ends of the ClpP cylinder. Although the pathway of substrate delivery is well established, the pathway of product release is unknown. Here, we show that the interface between the heptameric rings exchanges between two structurally distinct conformations. The conformational exchange process has been quantified by magnetization exchange experiments recorded between 0.5°C and 40°C, so that the thermodynamic properties for the transition could be obtained. Restriction of the observed motional freedom in ClpP through the introduction of a cysteine linkage results in a protease where substrate release becomes significantly slowed relative to the rate observed in the reduced enzyme, suggesting that the observed motions lead to the formation of transient side pores that may play an important role in product release.



# Quantitative Analysis of EXSY Spectra

Volume 214, number 2 CHEMICAL PHYSICS LETTERS 29 October 1993

#### NMR study of xenon dynamics and energetics in Na-A zeolite \*

R.G. Larsen, J. Shore, K. Schmidt-Rohr, L. Emsley, H. Long, A. Pines 1

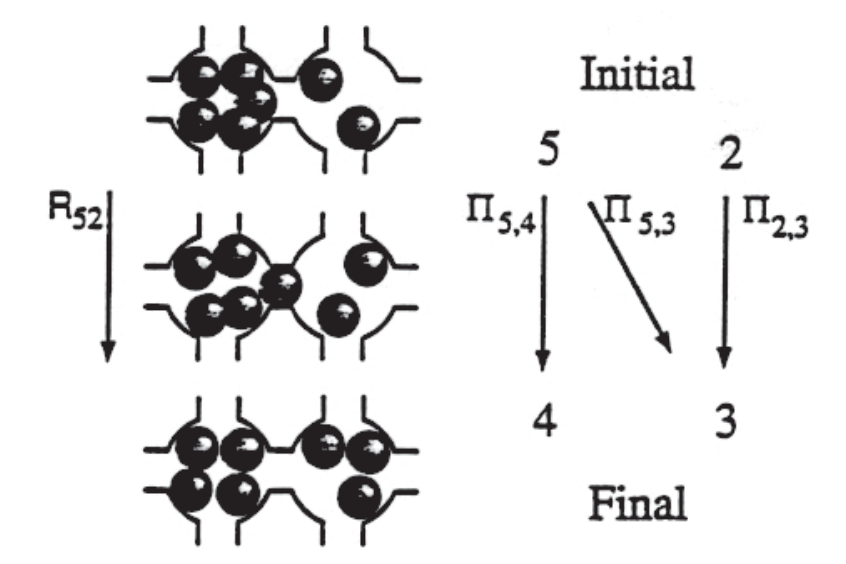
Materials Sciences Division, Lawrence Berkeley Laboratory, University of California, Berkeley, CA 94720, USA and Department of Chemistry, University of California, Berkeley, CA 94720, USA

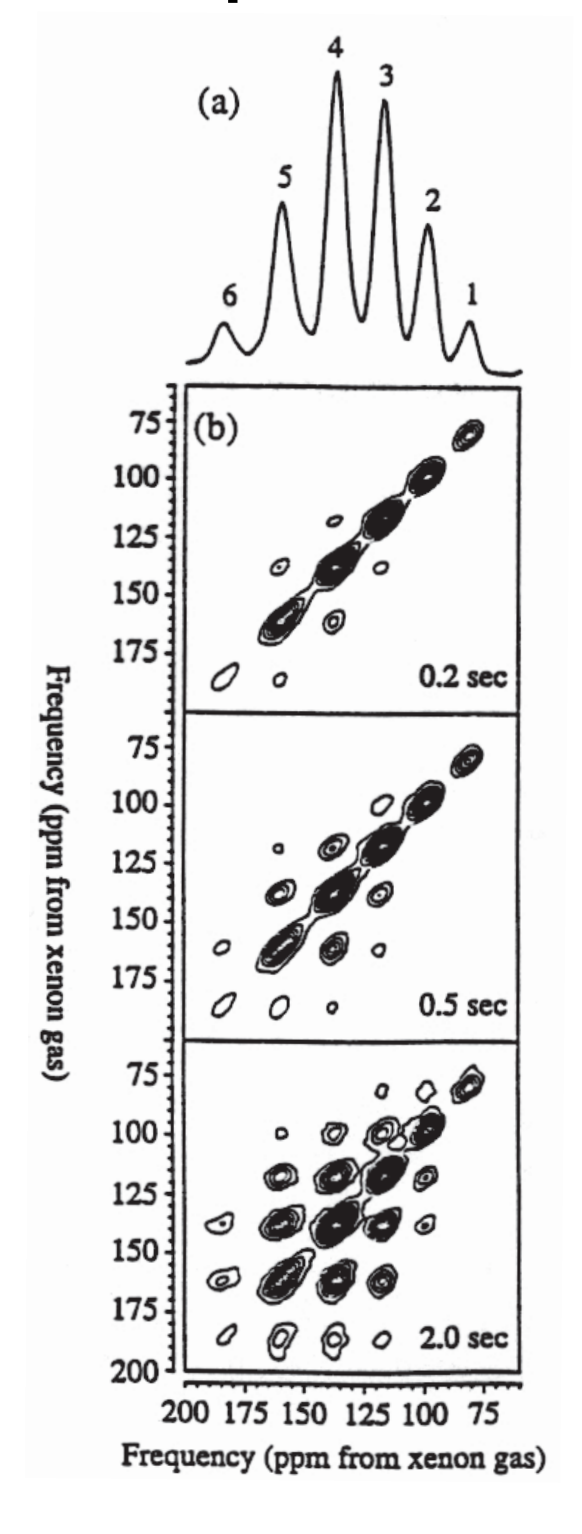
#### M. Janicke and B.F. Chmelka

Department of Chemical and Nuclear Engineering, University of California, Santa Barbara, CA 93106, USA

Received 18 June 1993

For xenon atoms adsorbed in Na-A zeolite, electronic interactions cause shifts in NMR frequencies, resulting in a spectrum with discrete peaks from xenon atoms in cages with different xenon occupancies. Using two-dimensional exchange NMR, it is possible to determine the microscopic rates of intercage motion and to relate them to the adsorption and activation energies of the xenon atoms. The dependence of the adsorption energies on xenon cage occupancy reflects the importance of the intracage interactions and is directly related to the cage occupancy distribution. Variable temperature measurements yield an activation energy of about 60 kJ/mol for the transfer of a xenon from one cage to another.





Homework: Read & Understand from this paper (pdf on Moodle) how one can go from the 2D exchange spectra to the activation energies

Name:

Correlation by:

EXSY (NOESY)

<sup>1</sup>H-<sup>1</sup>H exchange

COSY (DQF-COSY)

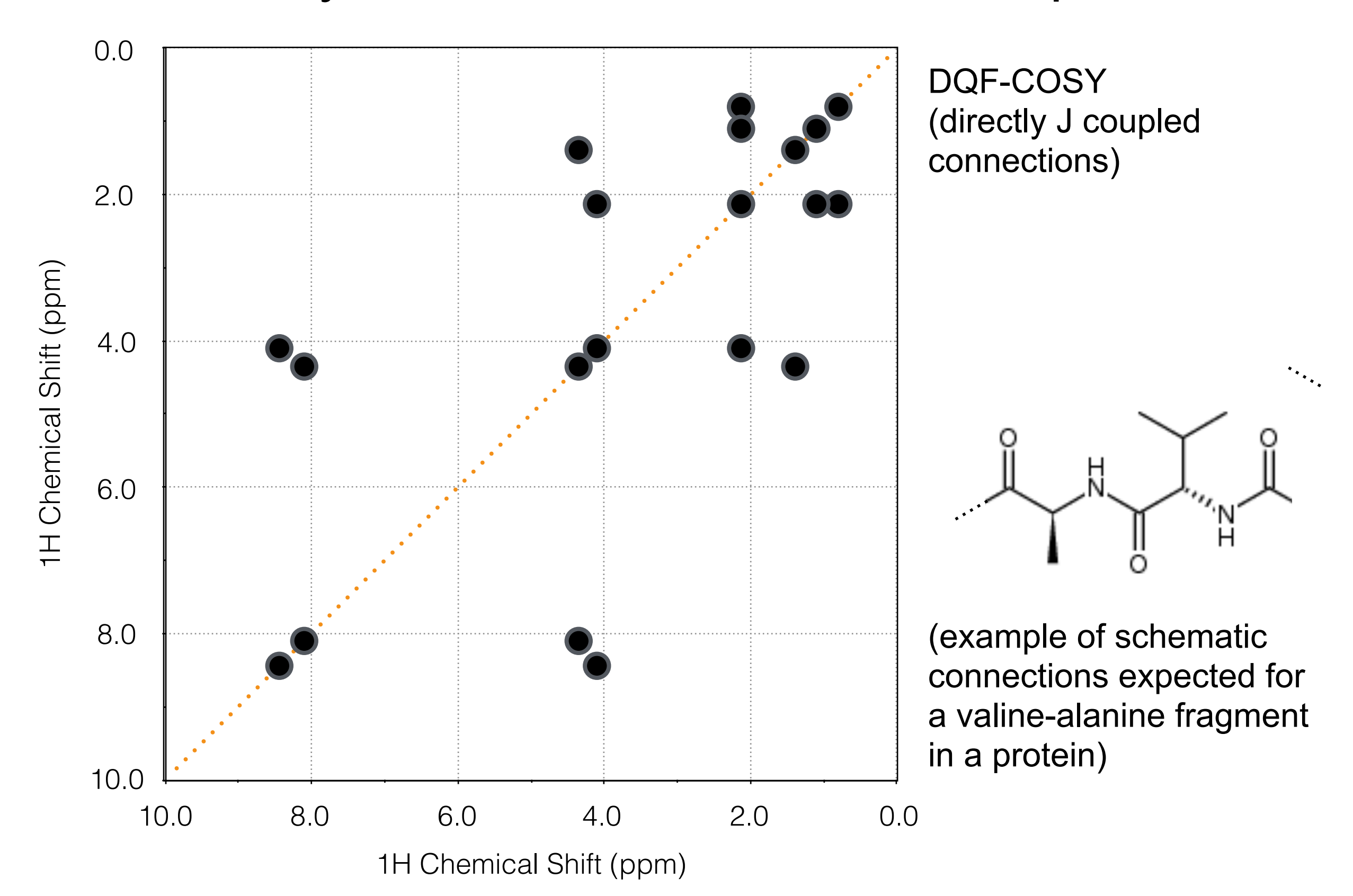
<sup>1</sup>H-<sup>1</sup>H Scalar Couplings (directly coupled spins only)

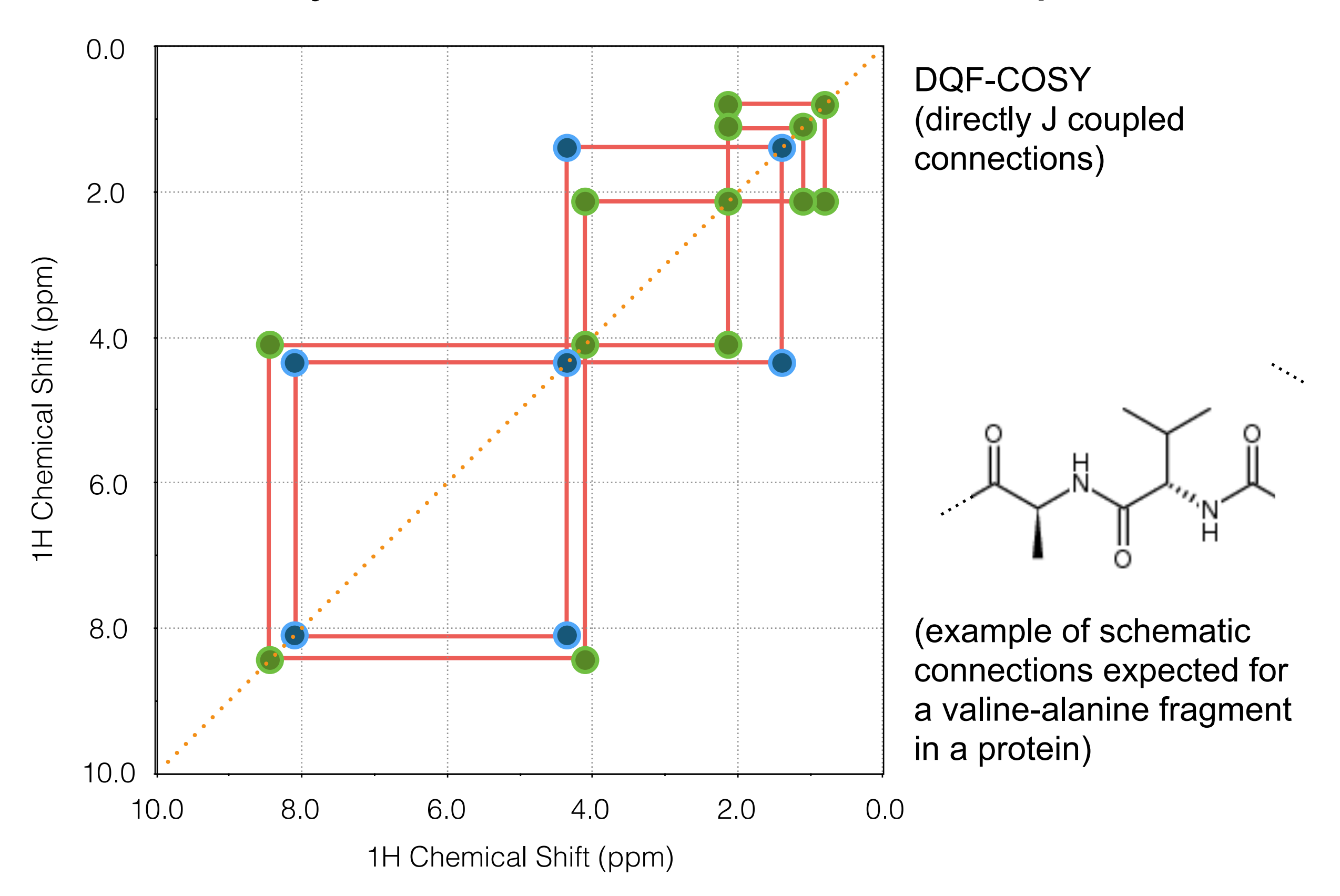
TOCSY

<sup>1</sup>H-<sup>1</sup>H Scalar Couplings (whole spin system)

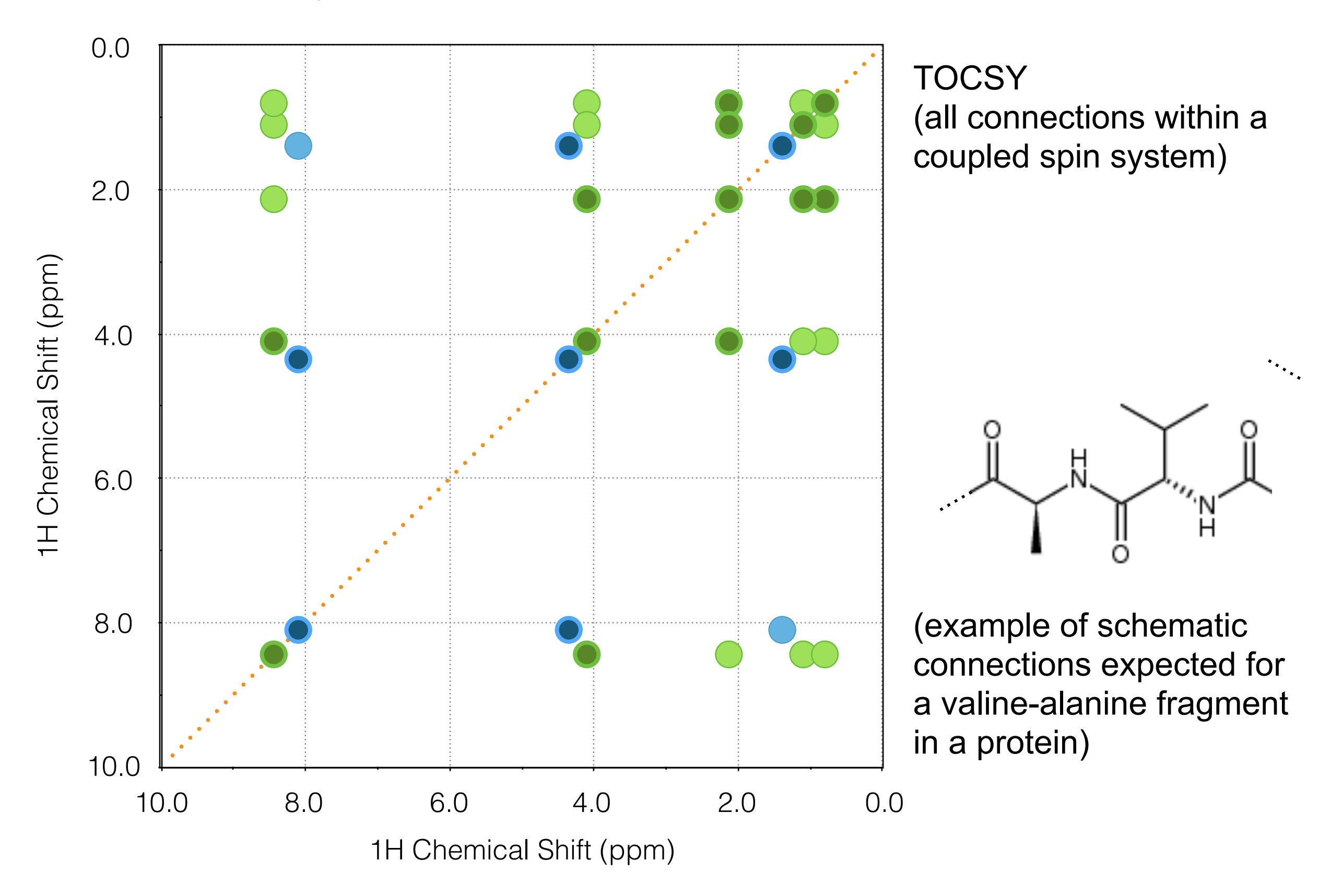
HSQC / HMQC

 ${}^{1}H-X {}^{1}J_{HX} Scalar couplings$ (X =  ${}^{13}C$ ,  ${}^{13}N$ ,  ${}^{13}P$ ,  ${}^{29}Si...$ )

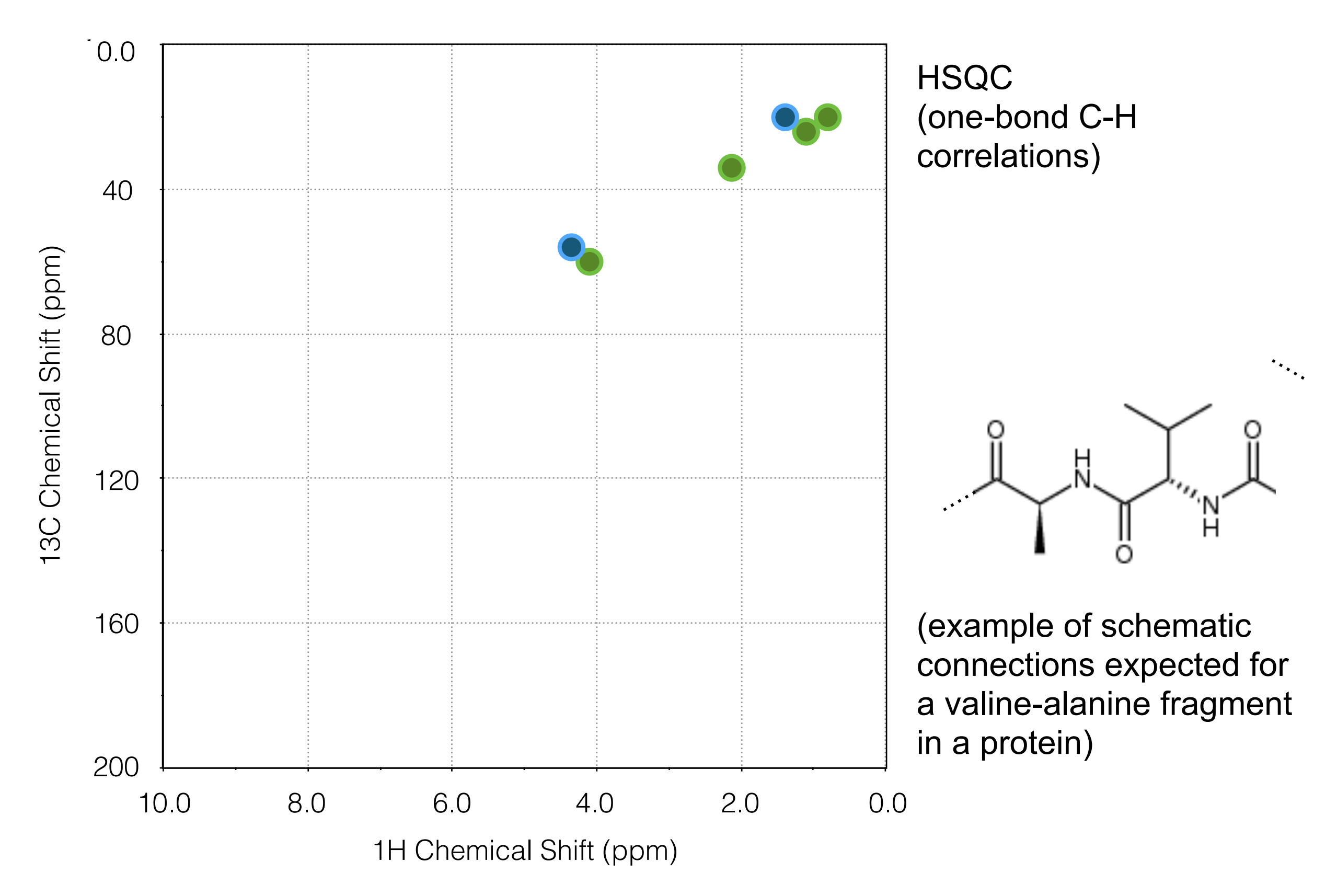




homework: assign the spectrum



homework: assign the spectrum



homework: assign the spectrum

# The Tip of the Iceberg....

46	TECHNIQUES							
Two- T	TABLE V HREE-, AND FOUR-DIMENSIONAL NMR EXPERIMEN	ıts						
Experiment cla								
(X = C  or  )		Ref.c						
$(t_1, t_2) = (H, H)$	COSY	(/)						

Experiment class <sup>a</sup> $(X = C \text{ or } N)$	Experiment*	Ref.		
$(t_1, t_2) = (H, H)$	COSY	(1)		
	RELAY	(2)		
	HOHAHA-TOCSY	(3)		
	NOESY	(4)		
	ROESY	(5)		
	DEPT-HMQC	(23)		
	DEPT-HMQC filtered TOCSY	(23)		
$(t_1, t_2, t_3) = (H, H, H)$	HOHAHA-NOESY	(6)		
$(t_1, t_2) = (X, H)$	HMQC	(7)		
(1, 2)	HSQC	(8)		
	CT-HSQC	(9)		
	HSMQC	(10)		
	НМВС	(11)		
	HETERO-RELAY	(12)		
	HETERO-NOE	(13)		
	H-X EXCSY	(14)		
$(t_1, t_2) = (C, C)$	CC-DQC	(15, 16		
(1), 12	CC-COSY	(16)		
	XX-EXCSY	(14)		
$(t_1, t_2) = (N, C)$	CN-MBC	(17)		
$(t_1, t_2, t_3) = (H, X, H)/(X, H, H)$	NOESY-HMOC	(18)		
(1, 2, 1)	нонана-нмос	(19)		
	SE-TOCSY-HSQC	(20)		
	SE-HSQC-TOCSY	(20)		
	SE-NOESY-HMQC	(20)		
	SE-NOESY-HSQC	(20)		
	HMQC-TOCSY	(21)		
	15N-TOCSY-NOESY	(22)		
	15N-NOESY-TOCSY	(22)		
	DEPT-TOCSY	(23)		
	HMQC-COSY (gradient)	(24)		
	NOESY-HMQC (gradient)	(25)		
$(t_1, t_2, t_3) = (H, C, H)$	HCCH-COSY	(26)		
(11213)	CT-HCCH-COSY	(27)		
	HCCH-TOCSY	(26)		
	HCCH-TOCSY (gradient)	(28)		
	H(CA)CO-TOCSY	(29)		
	H(CA)CO-COSY	(29)		
	(HCA)CO-CBHB	(29)		
	HA[CAN]HN	(30)		

[1] MULTINUCLEA	47							
TABLE V (continued)  Experiment class <sup>a</sup>								
$(t_1, t_2, t_3) = (C, C, H)$	НСАСО	(31)						
	CT-HCACO	(32)						
	C TOCSY-REVINEPT	(33)						
	H(N)CACO	(34)						
	<sup>13</sup> C- <sup>13</sup> C correlations	(35)						
	CBCACOHA (gradient)	(36)						
	CBCACOHA-TOCSY	(37)						
$(t_1, t_2, t_3) = (N, C, H)$	HNCO	(31)						
$(i_1, i_2, i_3) = (i_1, c, i_1)$	CT-HNCO	(38)						
	HNCA	(31, 39						
	CT-HNCA	(38)						
		(40, 41						
	HN(CO)CA	(38)						
	CT-HN(CO)CA							
	CT-HN(CA)CO	(42)						
	HNCO (gradient)	(43)						
$(t_1, t_2, t_3) = (C, N, H)$	HCA(CO)N	(31)						
	CT-HCA(CO)N	(32, 44)						
	CBCA(CO)NH	(45)						
	HNCACB	(46)						
	HC(CO)NH-TOCSY	(47)						
	HC(C)NH-TOCSY	(48)						
$(t_1, t_2, t_3) = (H, N, H)$	HA(CA)NNH	(49)						
	HN(CA)HA-GLY	(50)						
	HBHA(CO)NH	(51)						
	H(CCO)NH-TOCSY	(47)						
	HN(CA)NNH	(52)						
	HA[CAN]HN	(30)						
$(t_1, t_2, t_3) = (N, N, H)$	15N/15N edited 1H-1H NOESY	(53)						
	HN(CA)NNH	(52)						
$(t_1, t_2, t_3) = (N, H, H)$	HN(CA)HA	(54)						
(11.21.3)	HN(COCA)HA	(55)						
$(t_1, t_2, t_3, t_4) = (C, H, N, H)$	<sup>13</sup> C/ <sup>15</sup> N-edited <sup>1</sup> H- <sup>1</sup> H NOESY	(56)						
(1, 12, 13, 14) = (0, 11, 11, 11)	HNCAHA	(57)						
A STATE OF THE STA	HN(CO)CAHA	(57)						
$(t_1, t_2, t_3, t_4) = (H, C, N, H)$	HCANNH	(58)						
(11, 12, 13, 14) - (11, 0, 11, 11)	HCC(CO)NNH	(59)						
$(t_1, t_2, t_3, t_4) = (C, H, C, H)$	13C/13C-edited 1H-1H NOESY	(60)						
(1, 12, 13, 14) - (0, 11, 0, 11)	13C/13C 1H-1H NOESY (gradient)	(61)						
$(t_1, t_2, t_3, t_4) = (C, C, N, H)$	HCACON	(62)						
(11, 12, 13, 14) = (C, C, N, N)	HCCH-TOCSY	(63)						
$(t_1, t_2, t_3, t_4) = (H, C, C, H)$ $(t_1, t_2, t_3, t_4) = (H, N, N, H)$	HN(COCA)NH	(64)						

Pulse sequences are organized by the nuclei that are operative in the various acquisition periods. The number of time domains (i, values) establishes the dimensionality of the (continued)

# The Tip of the Iceberg....

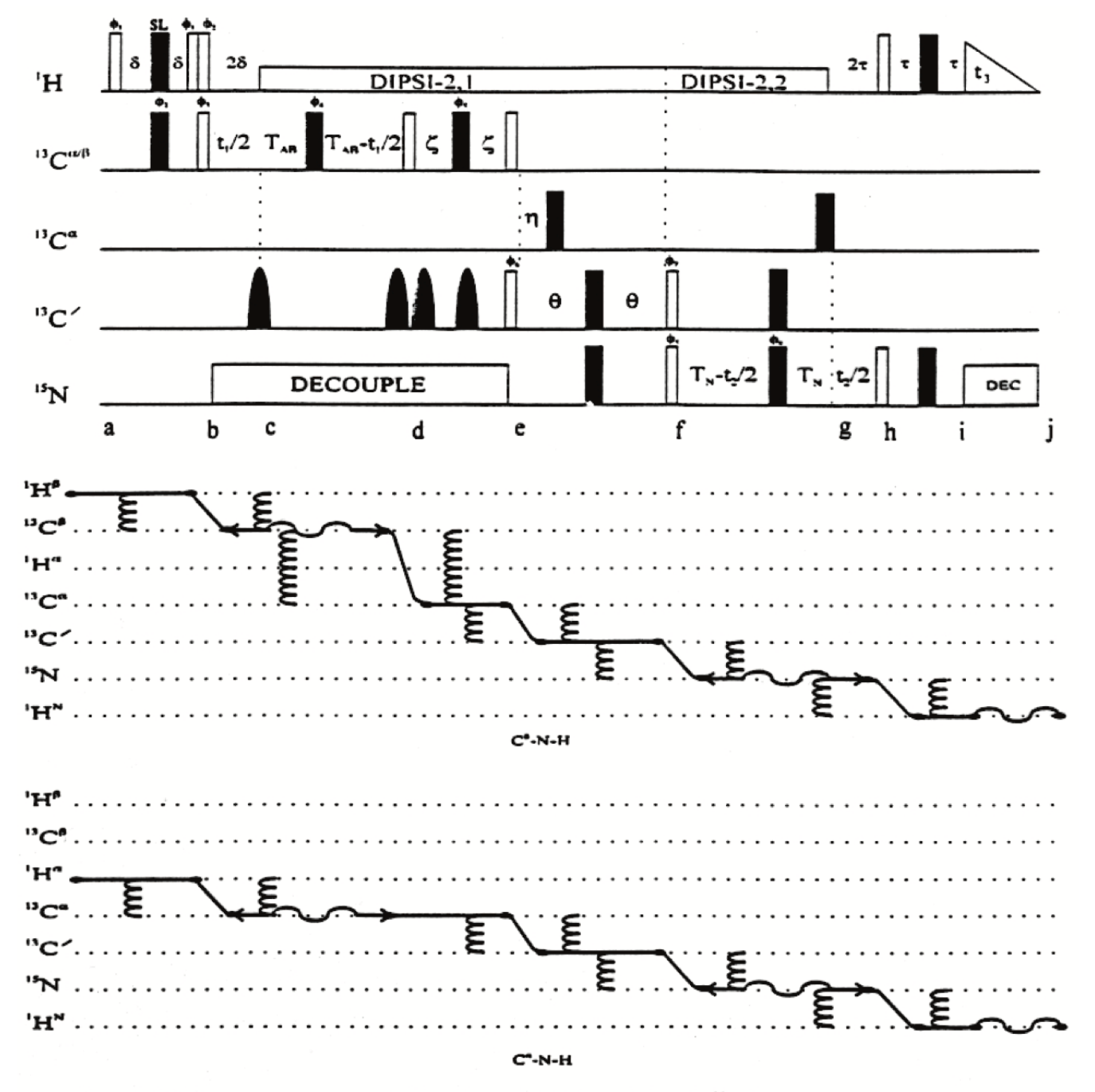


Fig. 14. Pulse sequence and CFN for 3D-CBCA(CO)NH.<sup>11</sup> The pulses and phases have the same convention described in Fig. 12. For values of the delays, consult the original work. The second and third selective (rounded) carbonyl pulses and the phase labeled  $\phi_7$  serve to remove nonresonant phase distortions (Section III.C). The CFN is best shown as two separate experiments, one originating from  $^1H^{\beta}$  and the second originating from  $^1H^{\alpha}$ .

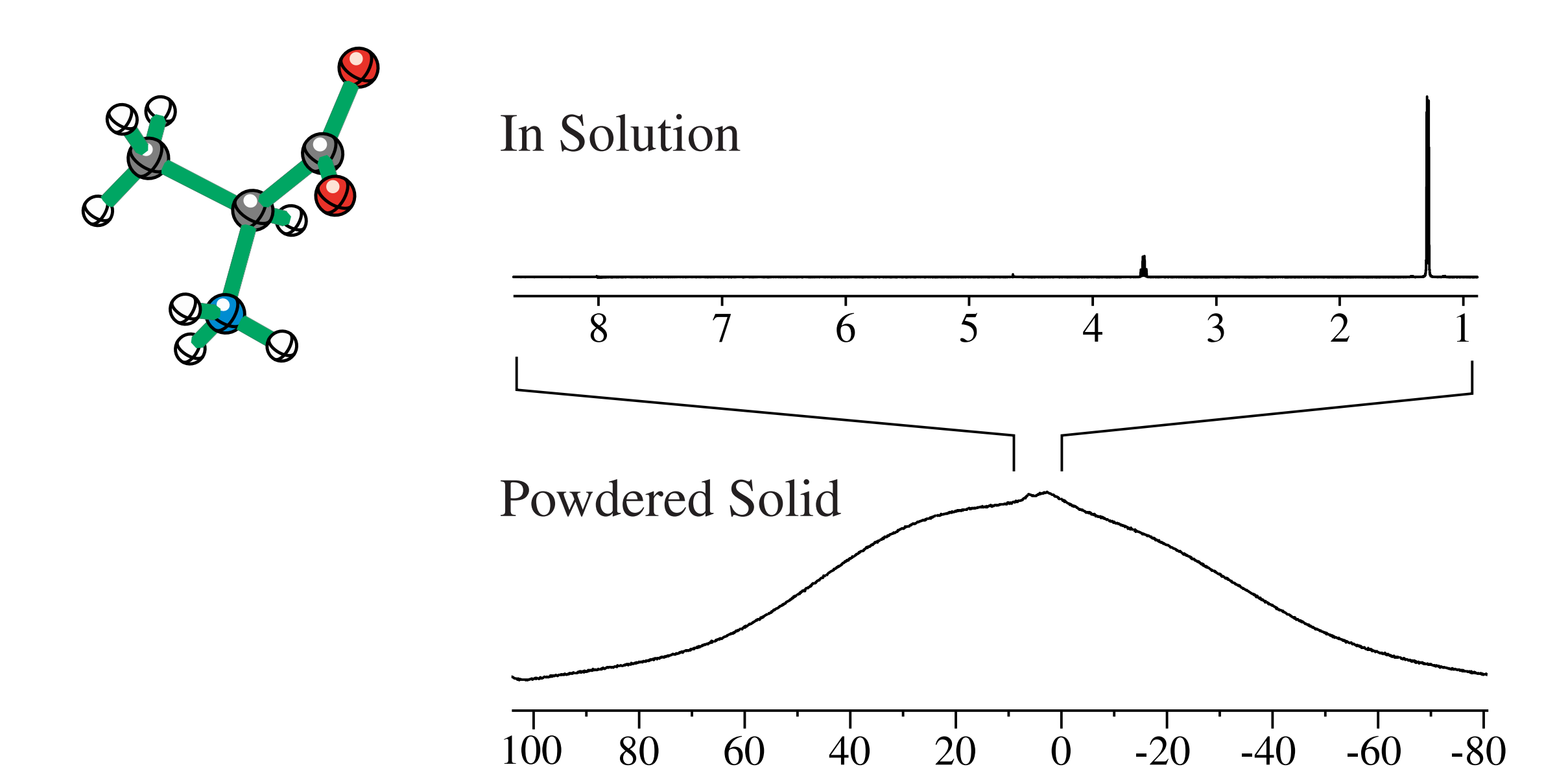
# Nuclear Magnetic Resonance

Week 4 NMR: Solid-state NMR

# Objectives

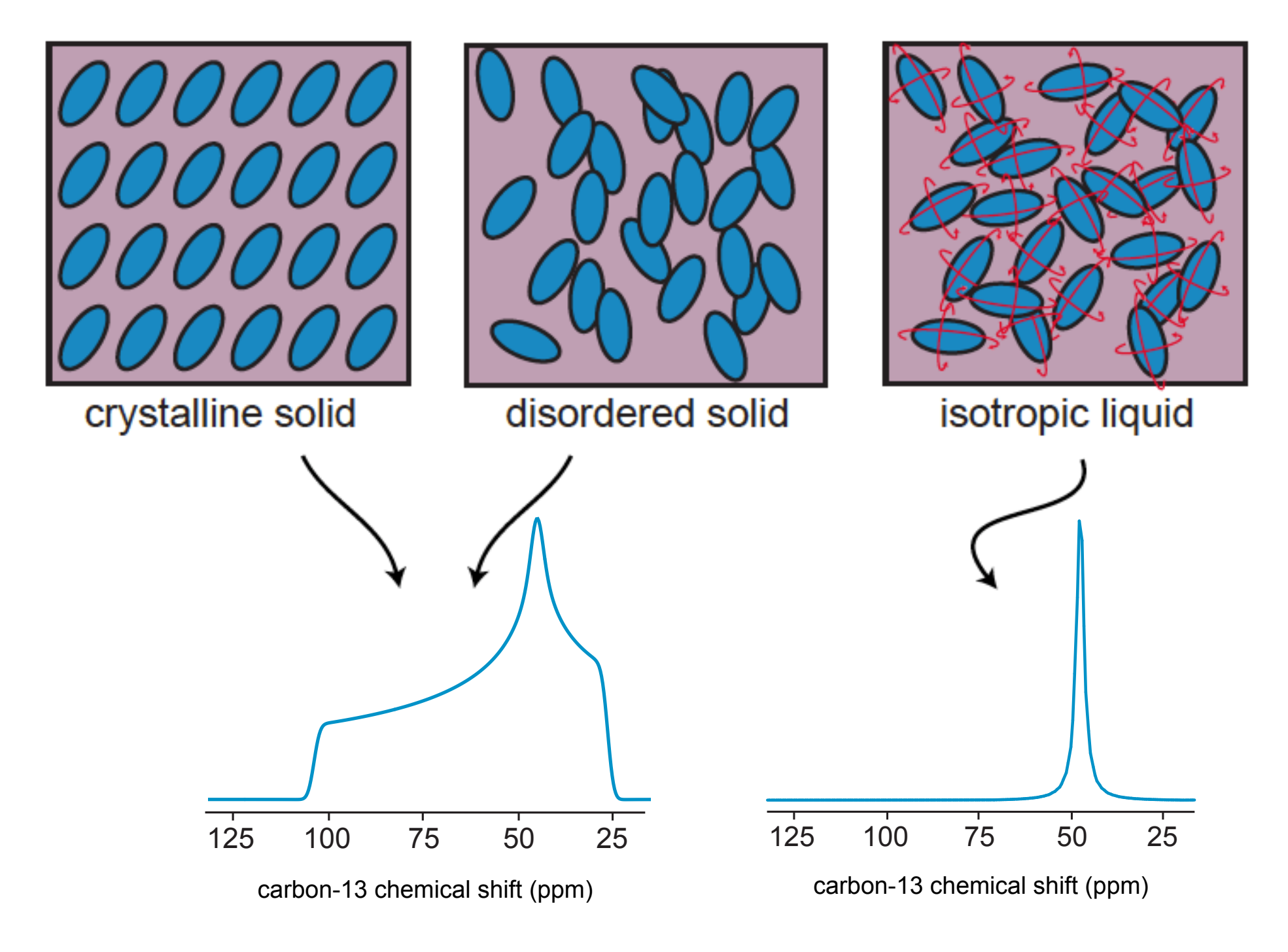
- Learn about anisotropy
- Learn about coherent averaging
- Know what MAS and spin decoupling are

### What's the Problem?

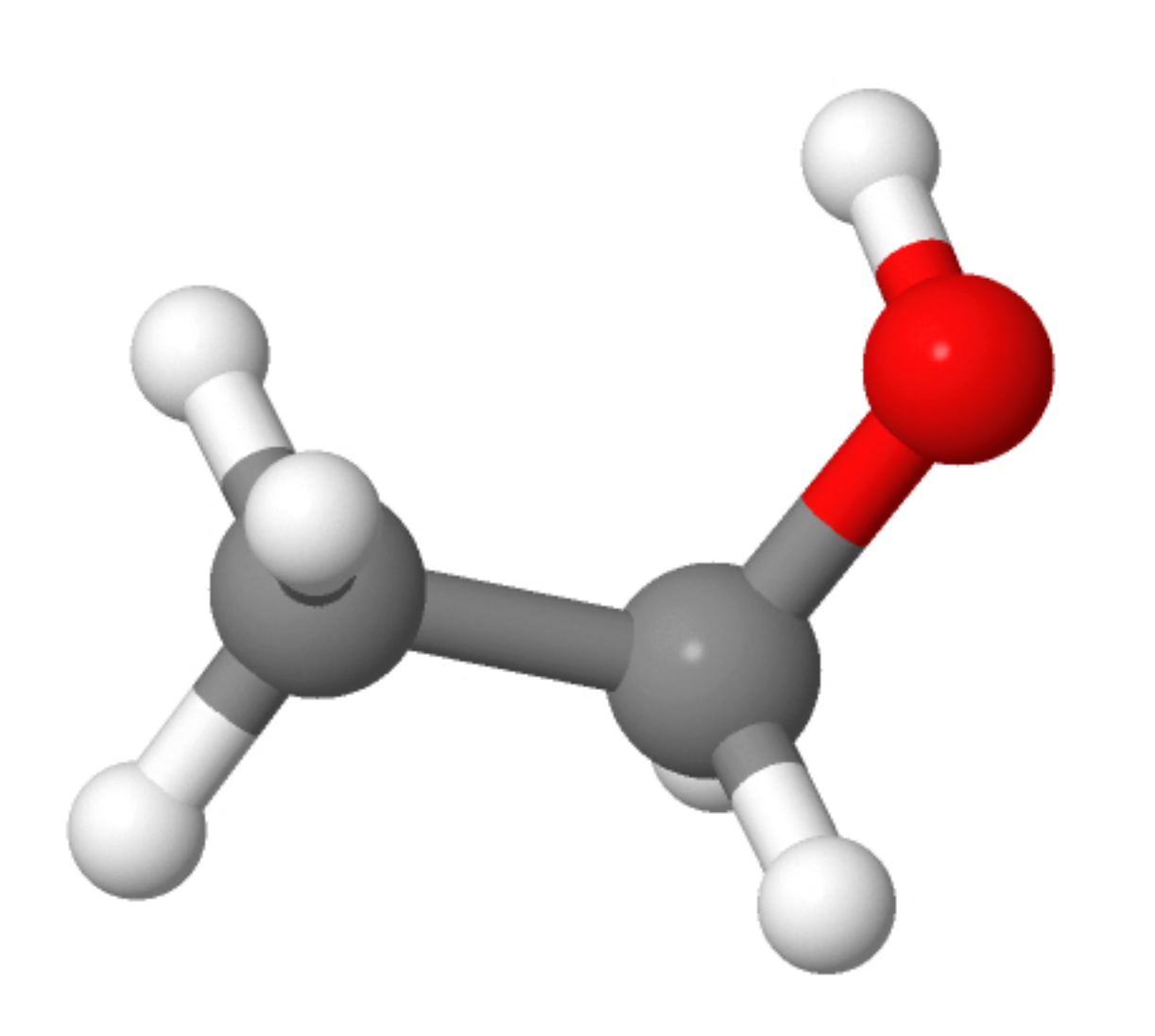


proton chemical shift (ppm)

# Solid-State NMR: Why is it different?



The only difference between solids and liquids, for NMR, is the presence or absence of rapid molecular motion.



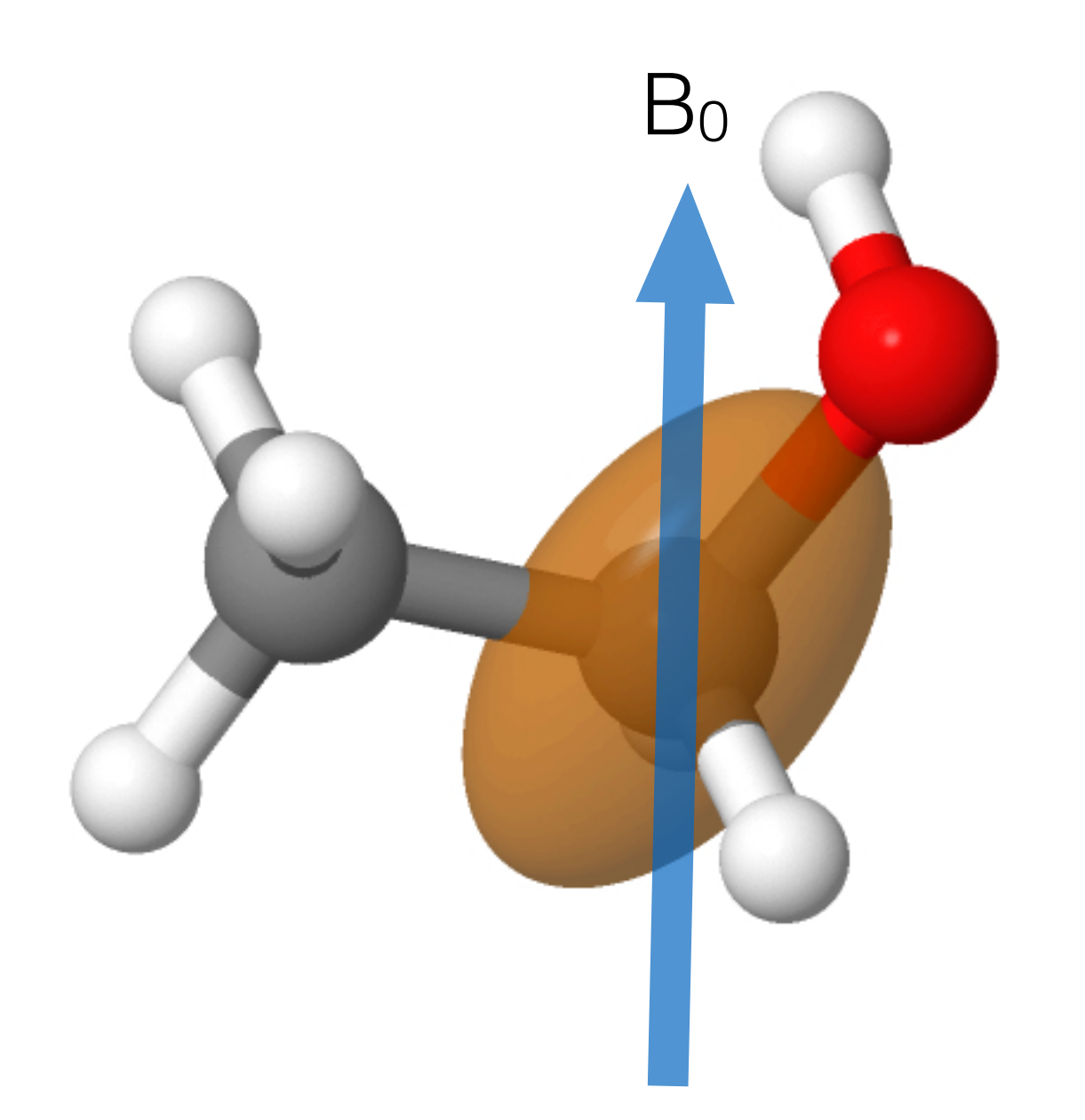
Consider the chemical shift of the CH<sub>2</sub> carbon resonance in ethanol

	s (l = 0)		p ( <i>l</i> = 1)		d (ℓ = 2)					f (l = 3)							
	m = 0	$0  m=0 \qquad m=\pm 1$		m = 0	$m = \pm 1$		$m = \pm 2$		m = 0	$m = \pm 1$		$m = \pm 2$		$m = \pm 3$			
	s	ρ <sub>z</sub>	ρ <sub>χ</sub>	ρ <sub>y</sub>	d <sub>z</sub> 2	d <sub>XZ</sub>	d <sub>yz</sub>	d <sub>xy</sub>	d <sub>x</sub> 2 <sub>-y</sub> 2	f <sub>z</sub> 3	f <sub>XZ</sub> 2	f <sub>yz</sub> 2	f <sub>xyz</sub>	$f_{Z(X^2-y^2)}$	$f_{\chi(\chi^2-3y^2)}$	$f_{y(3x^2-y^2)}$	
n = 1	•																
n = 2	•																
n = 3	•	3			-	*	8		<b>9</b>								
n = 4	•	3	••		-	*	2		••	*	*	*	*	*	•	•	
n = 5	•	3	••	<b>(</b>	*	*	2	(3)	••								
n = 6	•	3	••														
n = 7																	

The chemical shift can be thought of as the shielding of the nucleus from the external magnetic field by the electrons.

The magnetic field is a vector quantity (the magnetic field has a well defined direction). The electronic distribution around the nucleus is highly anisotropic.

Therefore the chemical shift must depend on the orientation of the molecule with respect to the magnetic field.

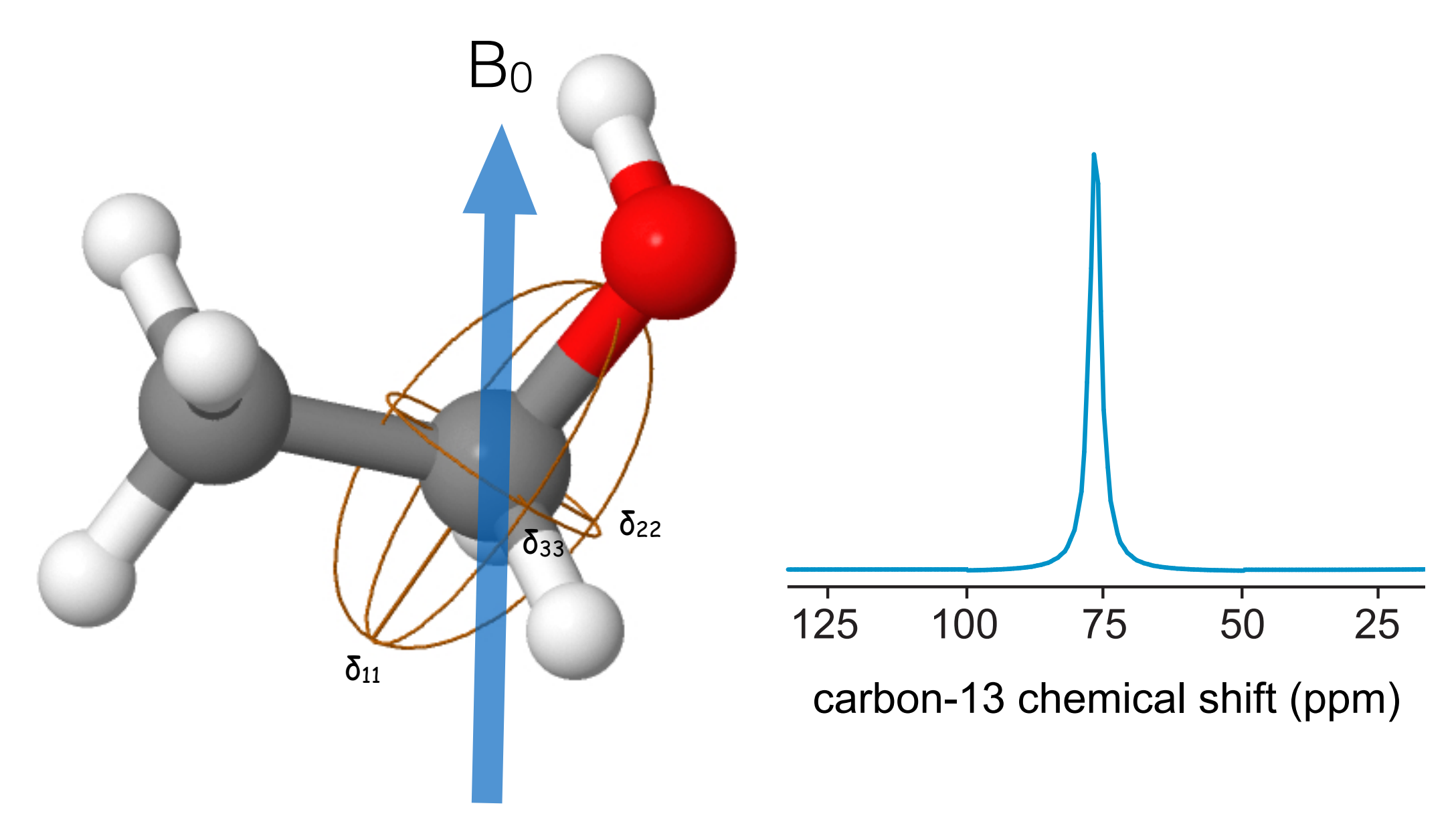


Here we represent the **chemical shift tensor** as (something like) an ellipsoid superimposed on the molecular structure.

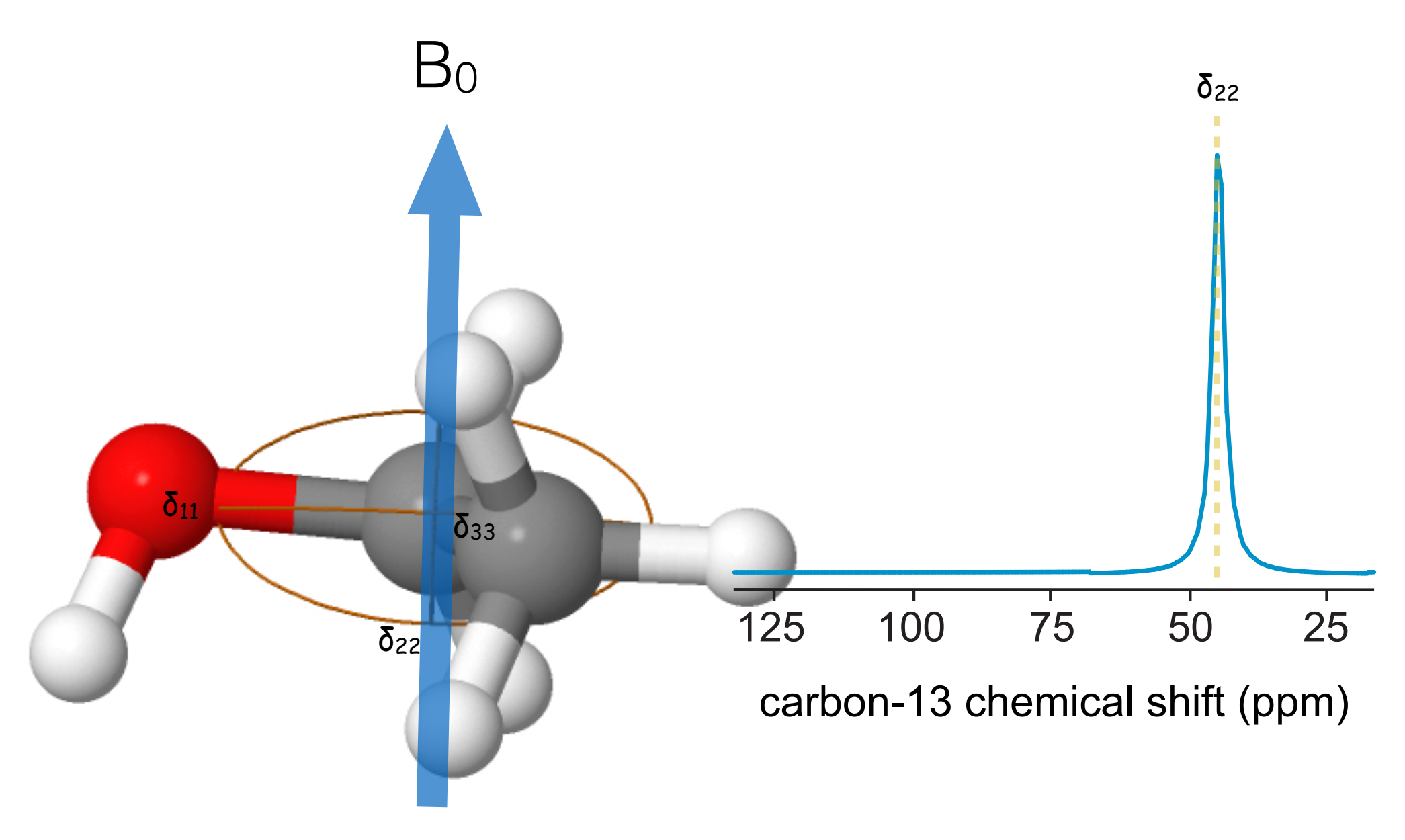
The shift tensor is fixed in the molecular frame.

Reminder: Shielding  $(\sigma)$  is related to chemical shift  $(\delta)$  by:

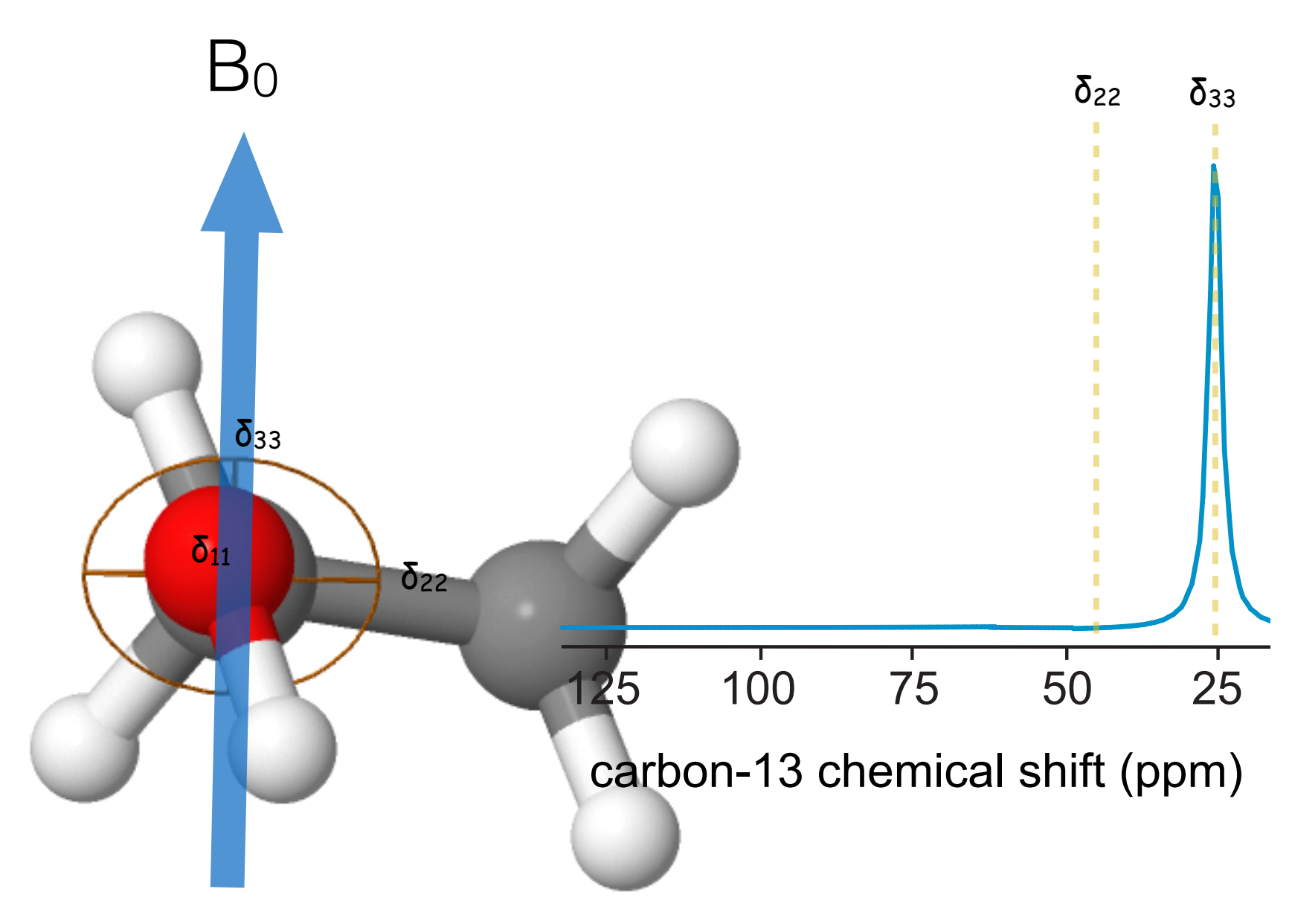
$$\delta \propto (1 - \sigma)$$



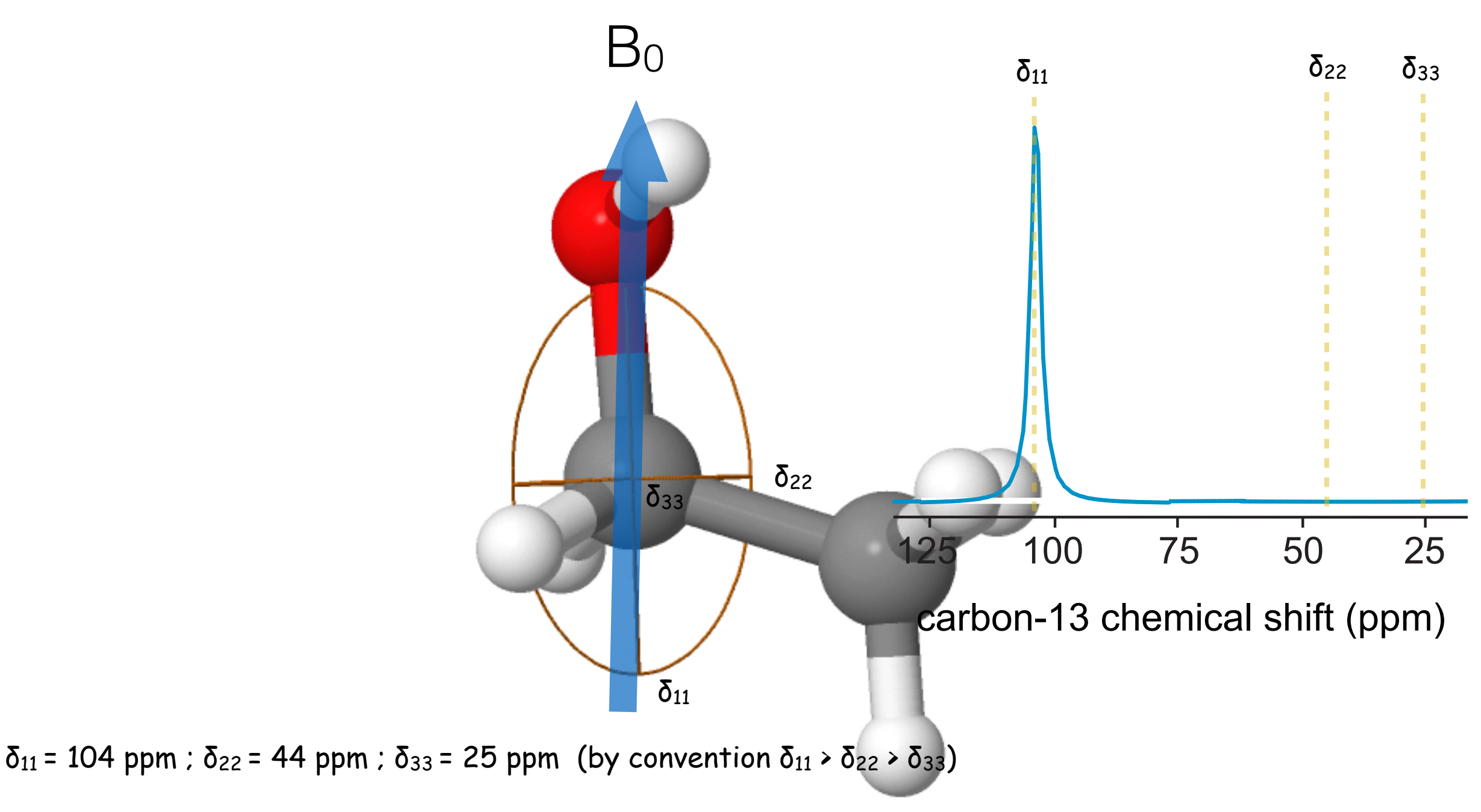
 $\delta_{11}$  = 104 ppm;  $\delta_{22}$  = 44 ppm;  $\delta_{33}$  = 25 ppm (by convention  $\delta_{11} > \delta_{22} > \delta_{33}$ )

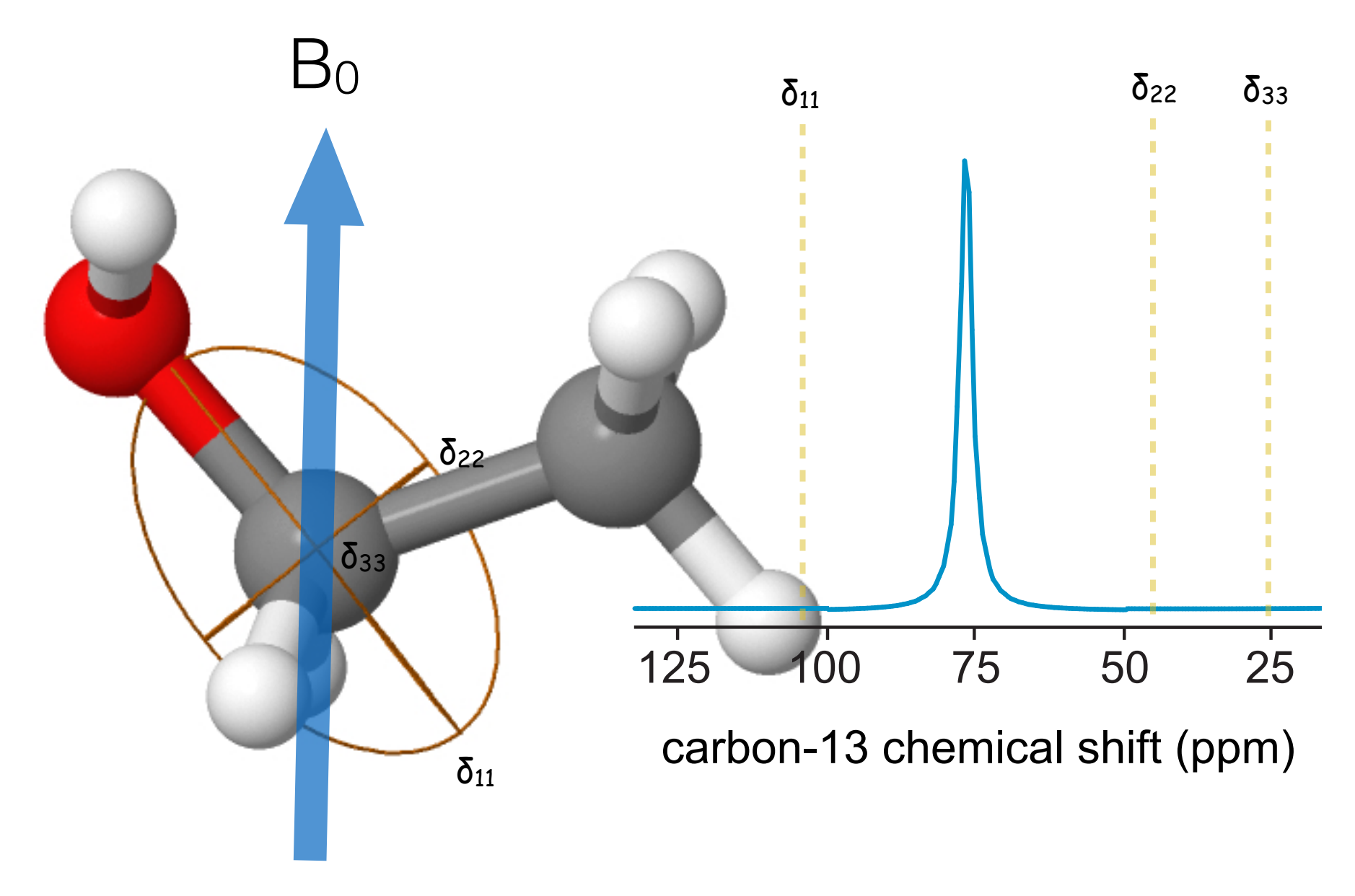


 $\delta_{11}$  = 104 ppm;  $\delta_{22}$  = 44 ppm;  $\delta_{33}$  = 25 ppm (by convention  $\delta_{11} > \delta_{22} > \delta_{33}$ )

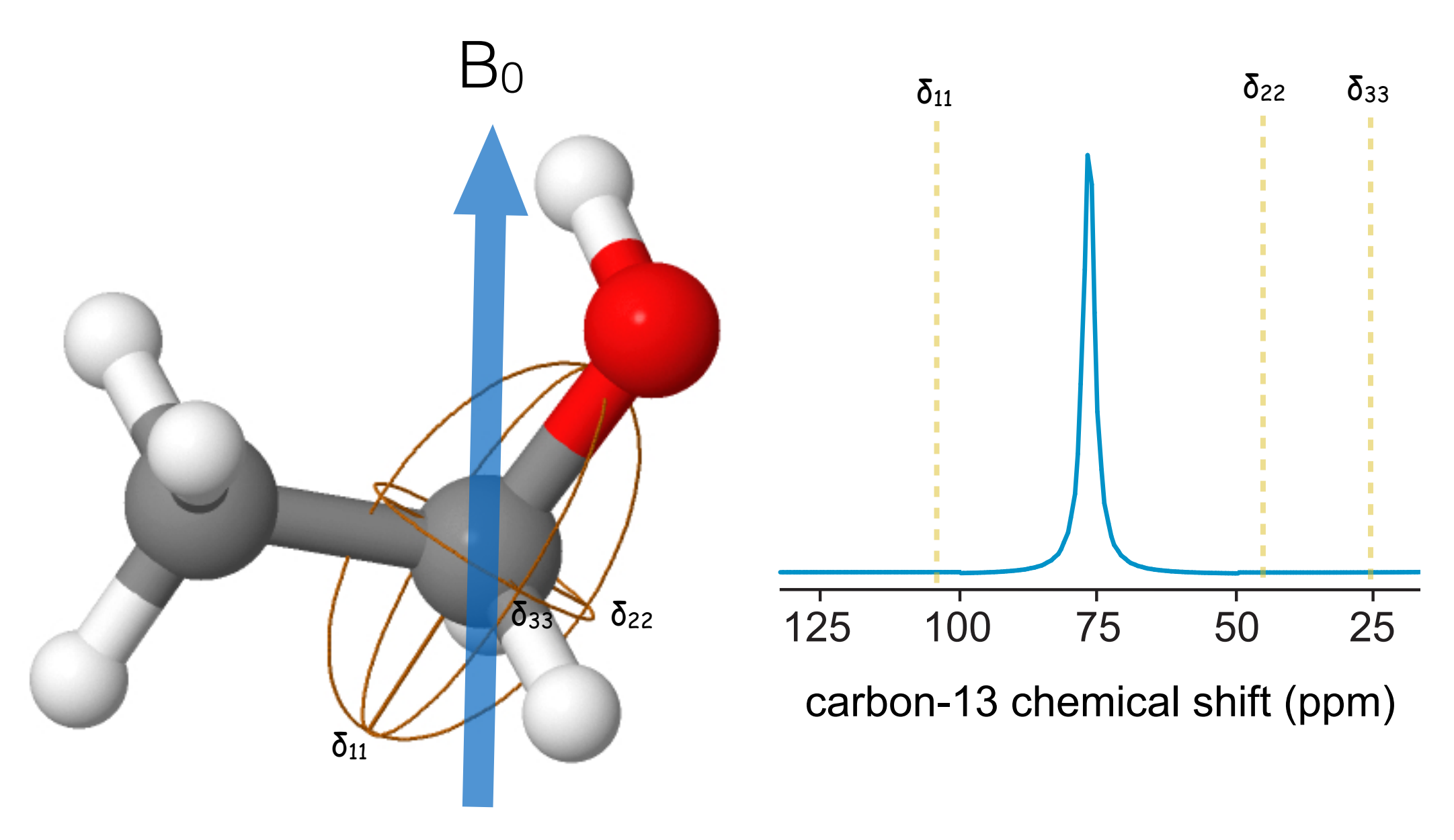


 $\delta_{11}$  = 104 ppm;  $\delta_{22}$  = 44 ppm;  $\delta_{33}$  = 25 ppm (by convention  $\delta_{11} > \delta_{22} > \delta_{33}$ )





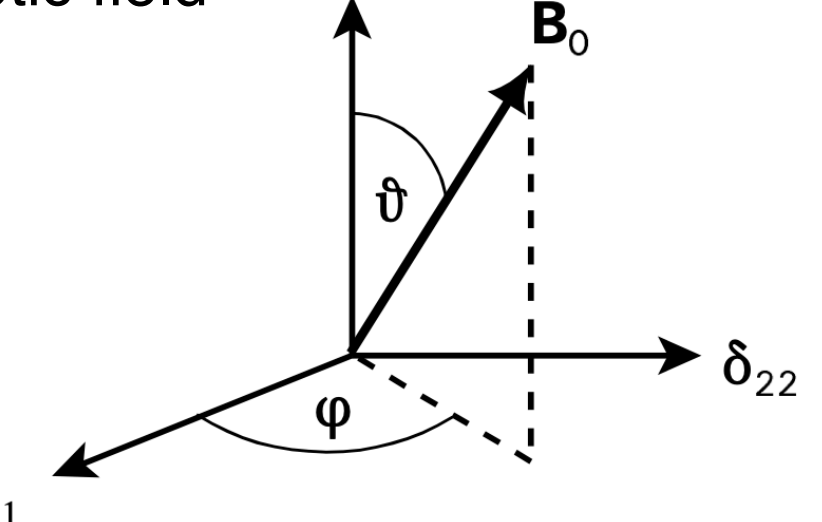
 $\delta_{11}$  = 104 ppm;  $\delta_{22}$  = 44 ppm;  $\delta_{33}$  = 25 ppm (by convention  $\delta_{11} > \delta_{22} > \delta_{33}$ )



 $\delta_{11}$  = 104 ppm;  $\delta_{22}$  = 44 ppm;  $\delta_{33}$  = 25 ppm (by convention  $\delta_{11} > \delta_{22} > \delta_{33}$ )

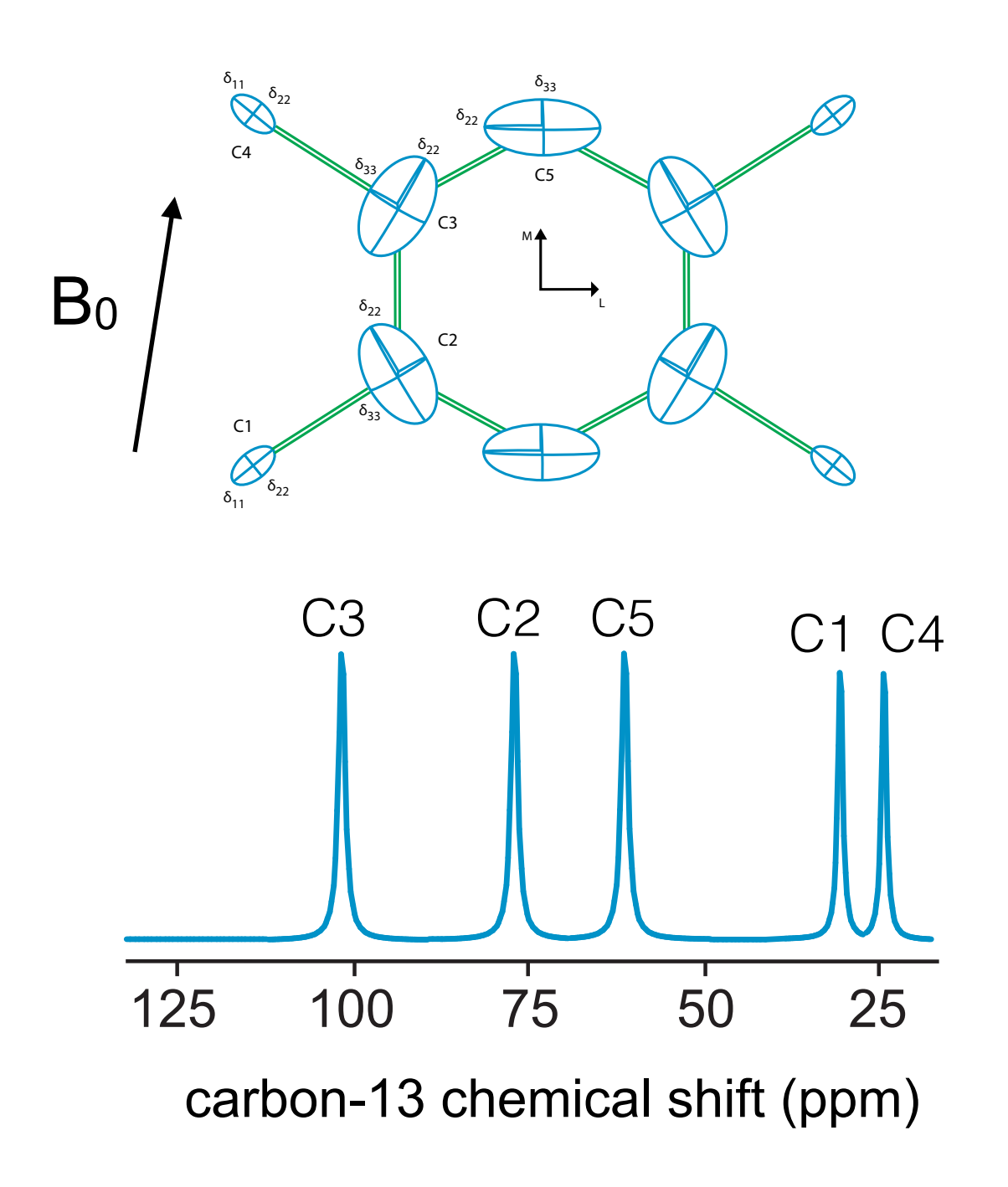
For any given orientation of the principle axis system of the chemical shift tensor with respect to the magnetic field the chemical shift is:

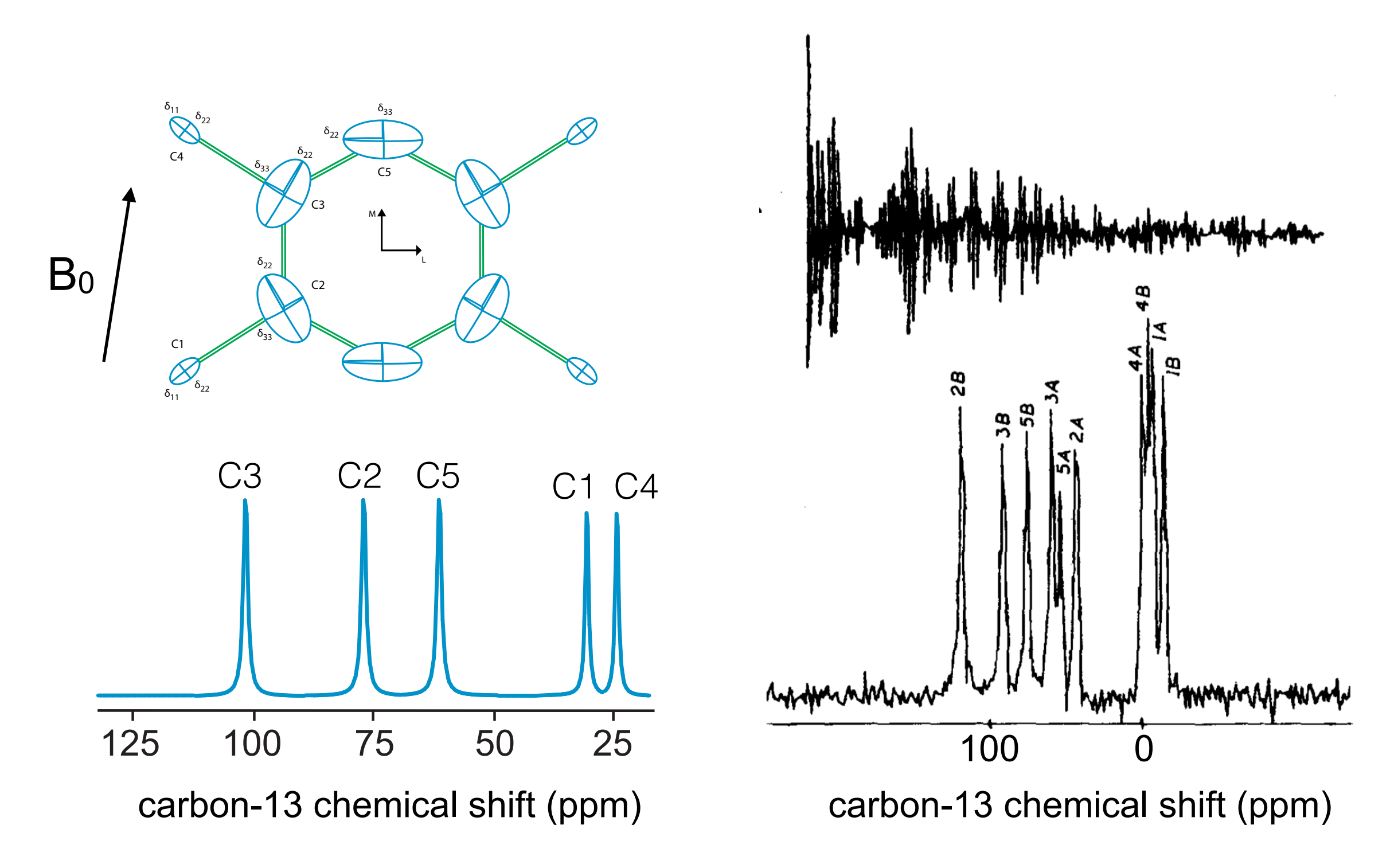
 $\delta(\theta, \phi) = \delta_{11} \sin^2\theta \cos^2\phi + \delta_{22} \sin^2\theta \sin^2\phi + \delta_{33} \cos^2\theta$ 



 $\delta_{33}$ 

What are the chemical shifts for a single crystal of durene at a given orientation?





Why are there 10 peaks in the experimental spectrum?

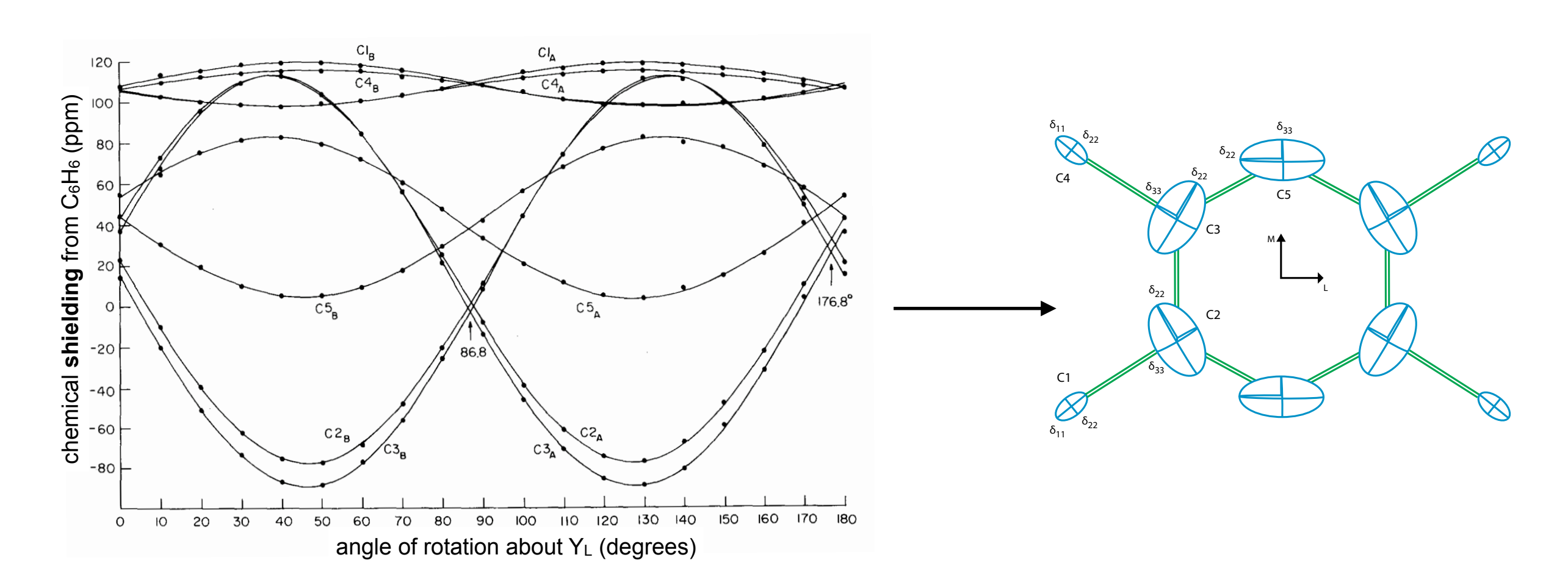
THE JOURNAL OF CHEMICAL PHYSICS

VOLUME 59, NUMBER 2

15 JULY 1973

#### Carbon-13 chemical shielding tensors in single-crystal durene\*

S. Pausak, A. Pines<sup>†</sup>, and J. S. Waugh
Department of Chemistry and Research Laboratory of Electronics,
Massachusetts Institute of Technology, Cambridge, Massachusetts 02139



The principle values and orientations of the chemical shift tensors (with respect to an external axes) can be obtained from a **rotation plot**. Chemical shifts are measured as a function of the crystal orientation as it is rotated around the x, y, and z axes in the laboratory.

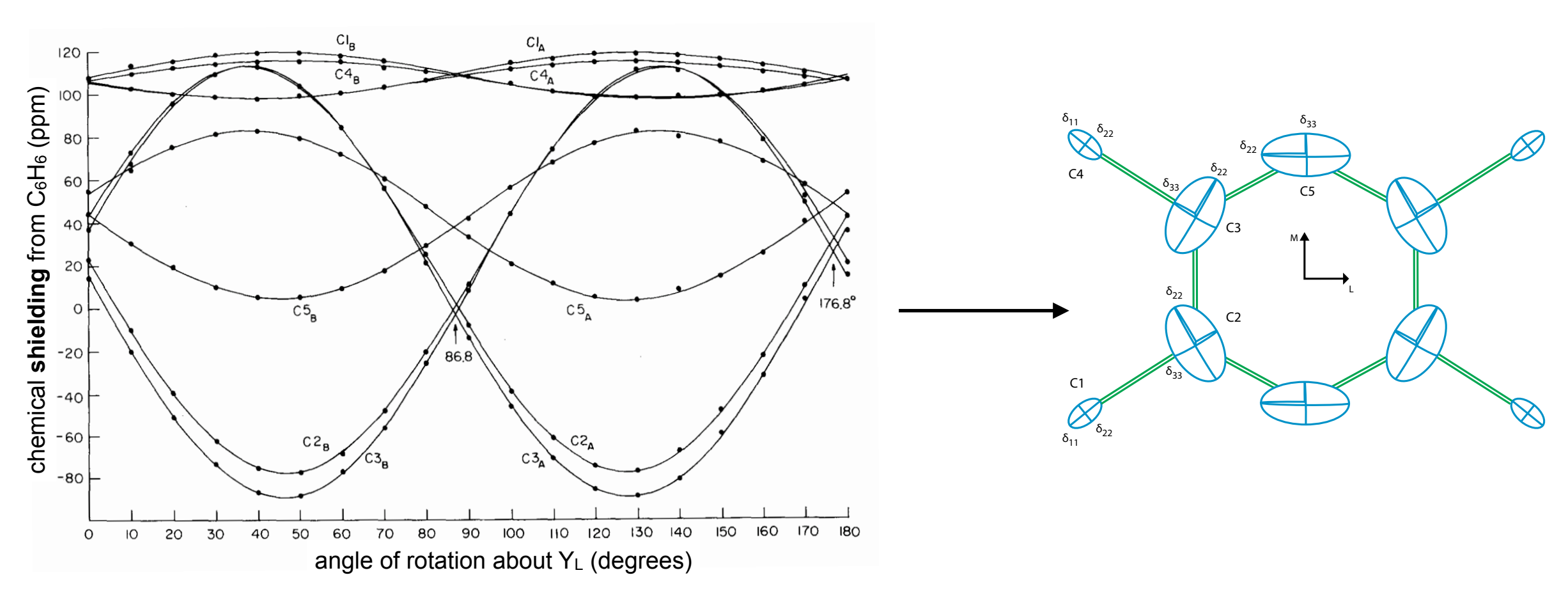
THE JOURNAL OF CHEMICAL PHYSICS

VOLUME 59, NUMBER 2

15 JULY 1973

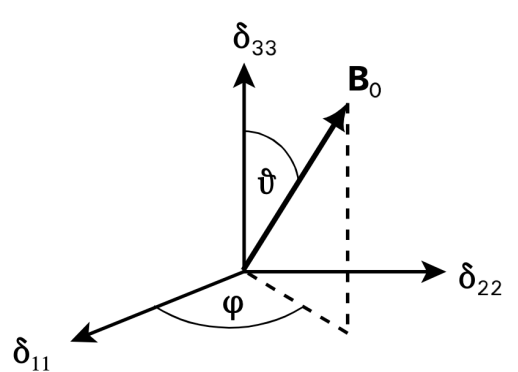
#### Carbon-13 chemical shielding tensors in single-crystal durene\*

S. Pausak, A. Pines<sup>†</sup>, and J. S. Waugh
Department of Chemistry and Research Laboratory of Electronics,
Massachusetts Institute of Technology, Cambridge, Massachusetts 02139



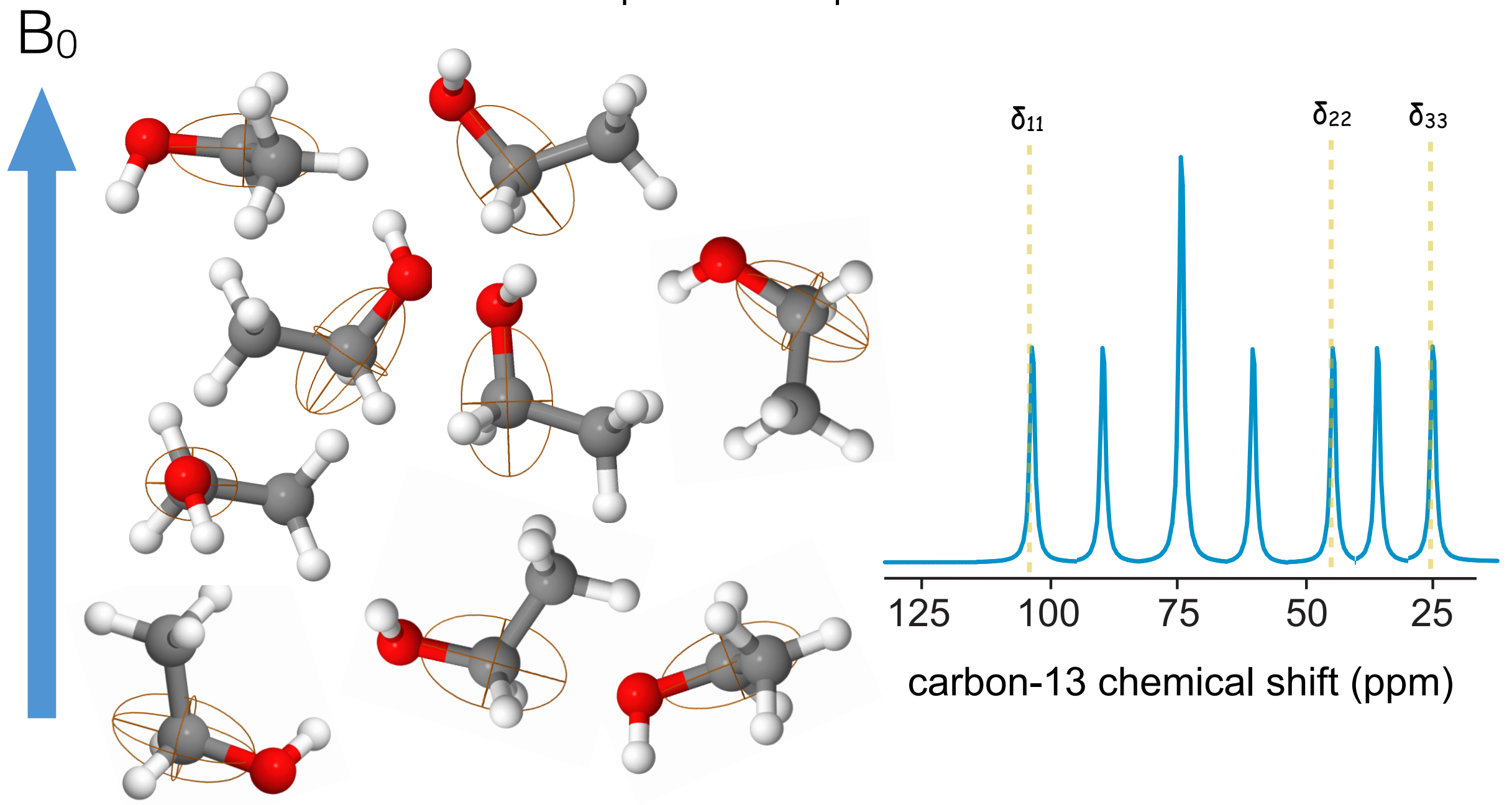
The chemical shift is a second rank spatial tensor property. (It therefore has the same orientation dependence as d-orbitals.)

$$\delta(\theta, \varphi) = \delta_{11} \sin^2\theta \cos^2\varphi + \delta_{22} \sin^2\theta \sin^2\varphi + \delta_{33} \cos^2\theta$$

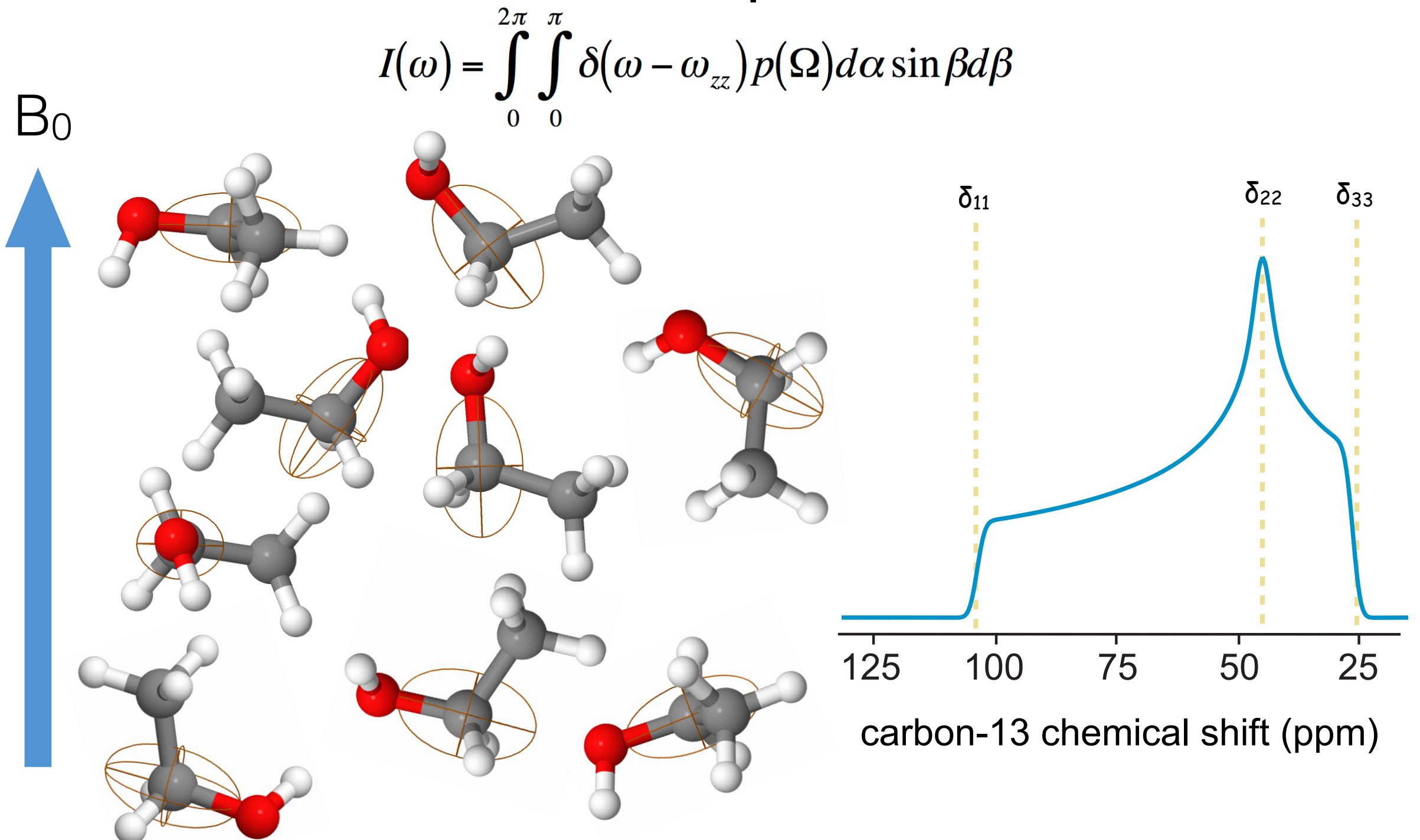


# Powder Spectra

What does the spectrum of a powder look like?



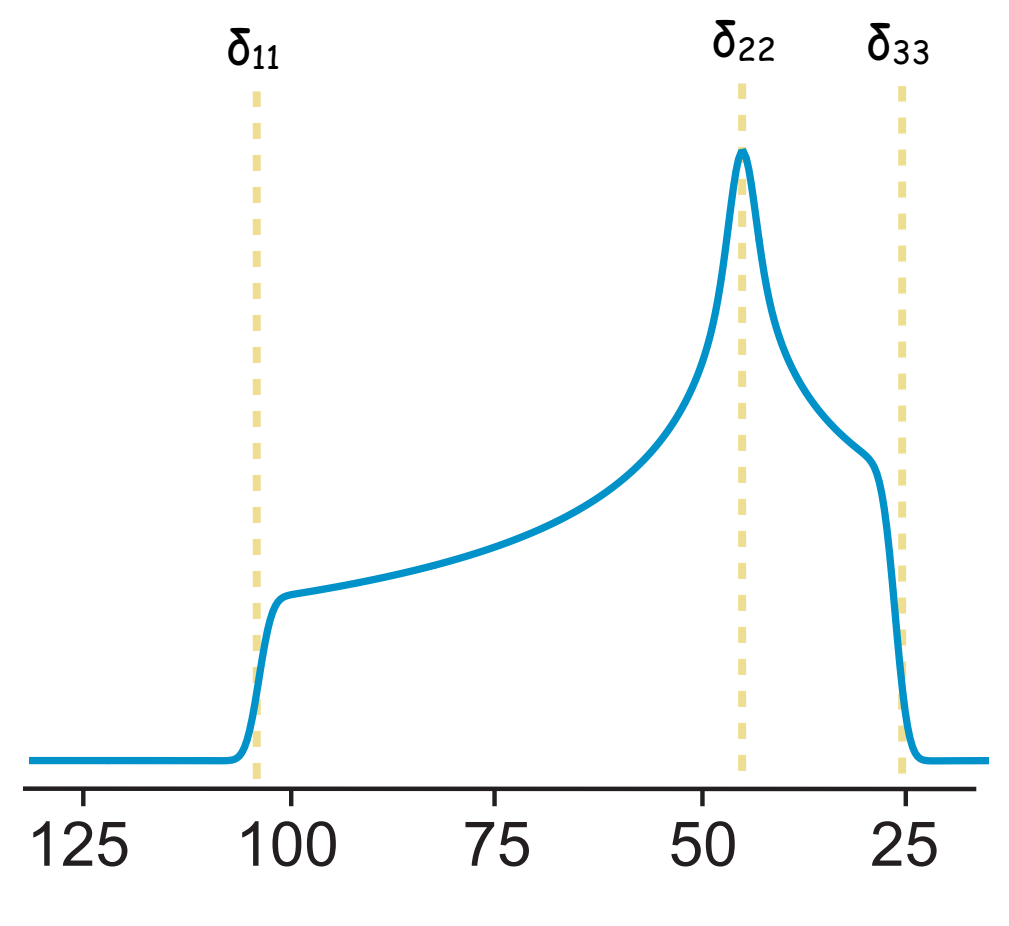
## Powder Spectra



 $p(\Omega)$  is the probability of finding a particular crystallite orientation and  $\omega_{zz}$  is the observed frequency for that orientation. In a powder sample, all orientations are present with equal probability. The spectrum of a powder is a sum of the spectra arising from each of the crystallites present in the sample.

## Powder Spectra

$$I(\omega) = \int_{0}^{2\pi} \int_{0}^{\pi} \delta(\omega - \omega_{zz}) p(\Omega) d\alpha \sin \beta d\beta$$



carbon-13 chemical shift (ppm)

Chemical shift principle values (but not orientations) are available from powder spectra by simple inspection.

# Powder Spectra

Chemical shift principle values (but not orientations) are available from powder spectra by simple inspection.

We refer to the special cases where  $\delta_{11} = \delta_{22}$  or  $\delta_{22} = \delta_{33}$  as **axially symmetric** tensors.

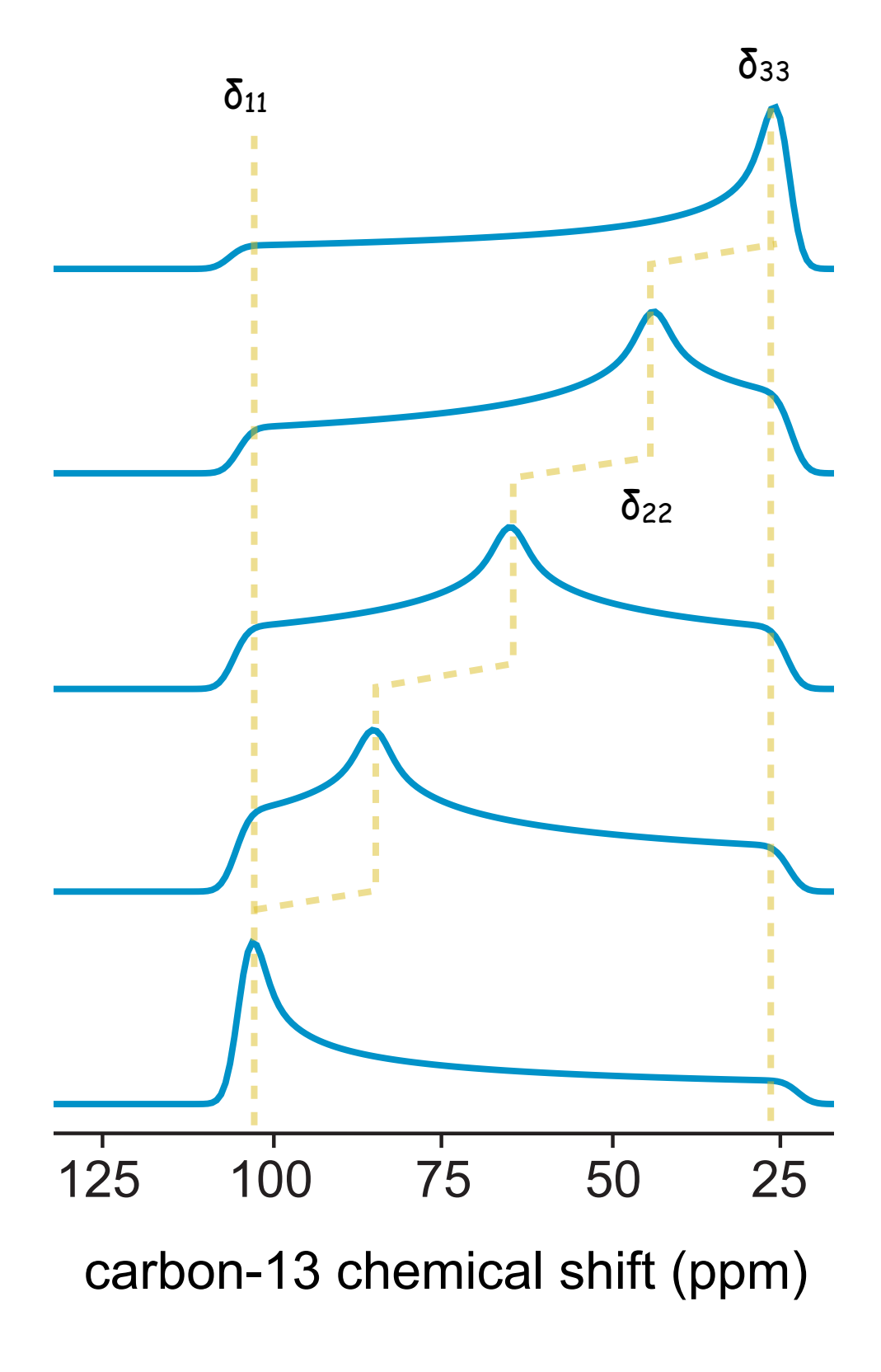
The CSA tensor principle values are often expressed in terms of the isotropic shift,  $\delta_{iso}$ , span,  $\Omega$ , and skew,  $\kappa$ :

$$\delta_{iso} = (\delta_{11} + \delta_{22} + \delta_{33})/3$$

$$\Omega = \delta_{11} - \delta_{33}$$

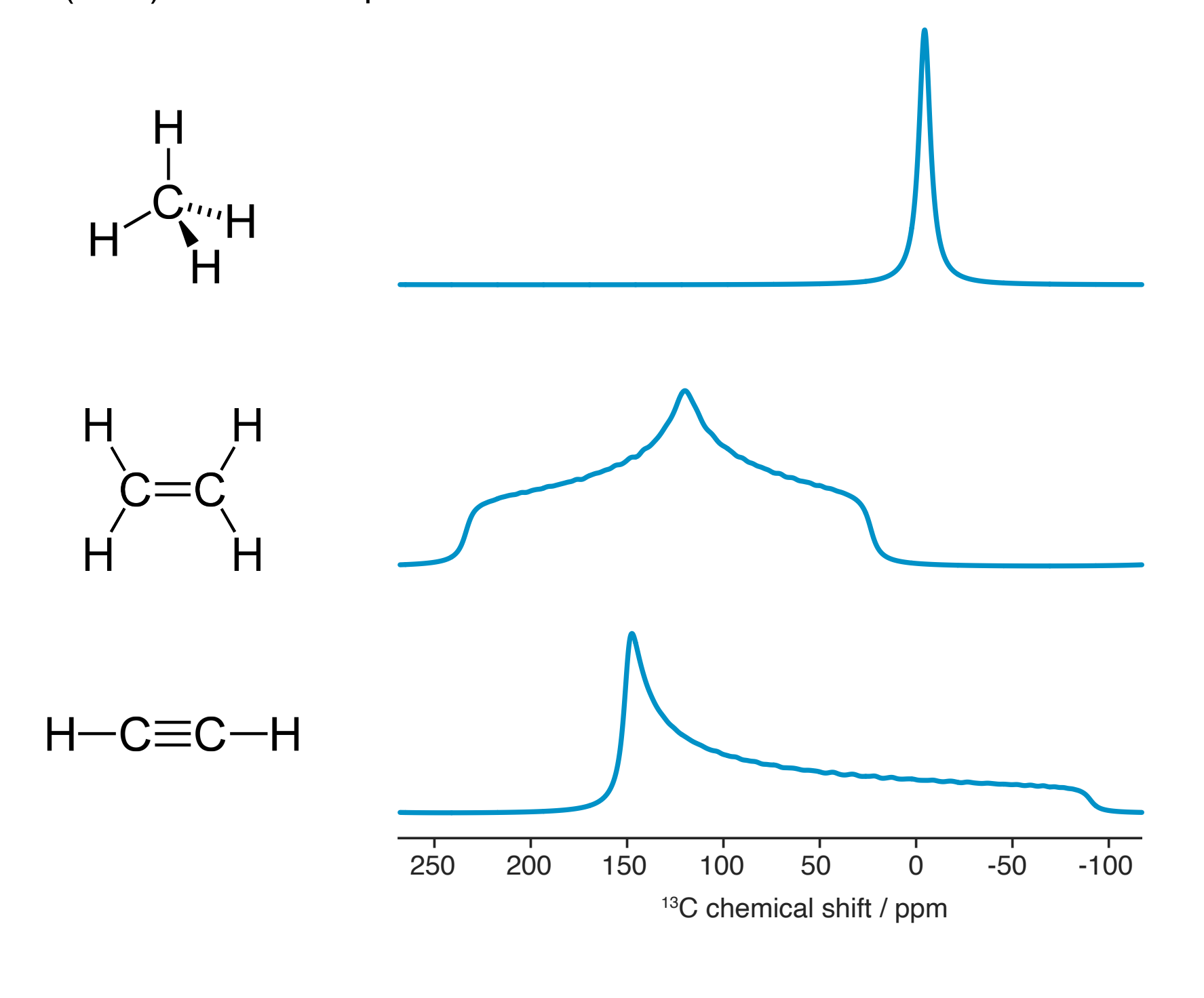
$$\kappa = 3(\delta_{22} - \delta_{iso})/\Omega$$

 $\Omega$  will always be larger than or equal to 0. It measures the overall extent of anisotropy.  $\kappa$  will range from -1 to 1 and it measures the deviation from axial symmetry.



# **Chemical Shift Anisotropy**

Consider carbon-13 chemical shift anisotropy (CSA) in some simple cases:

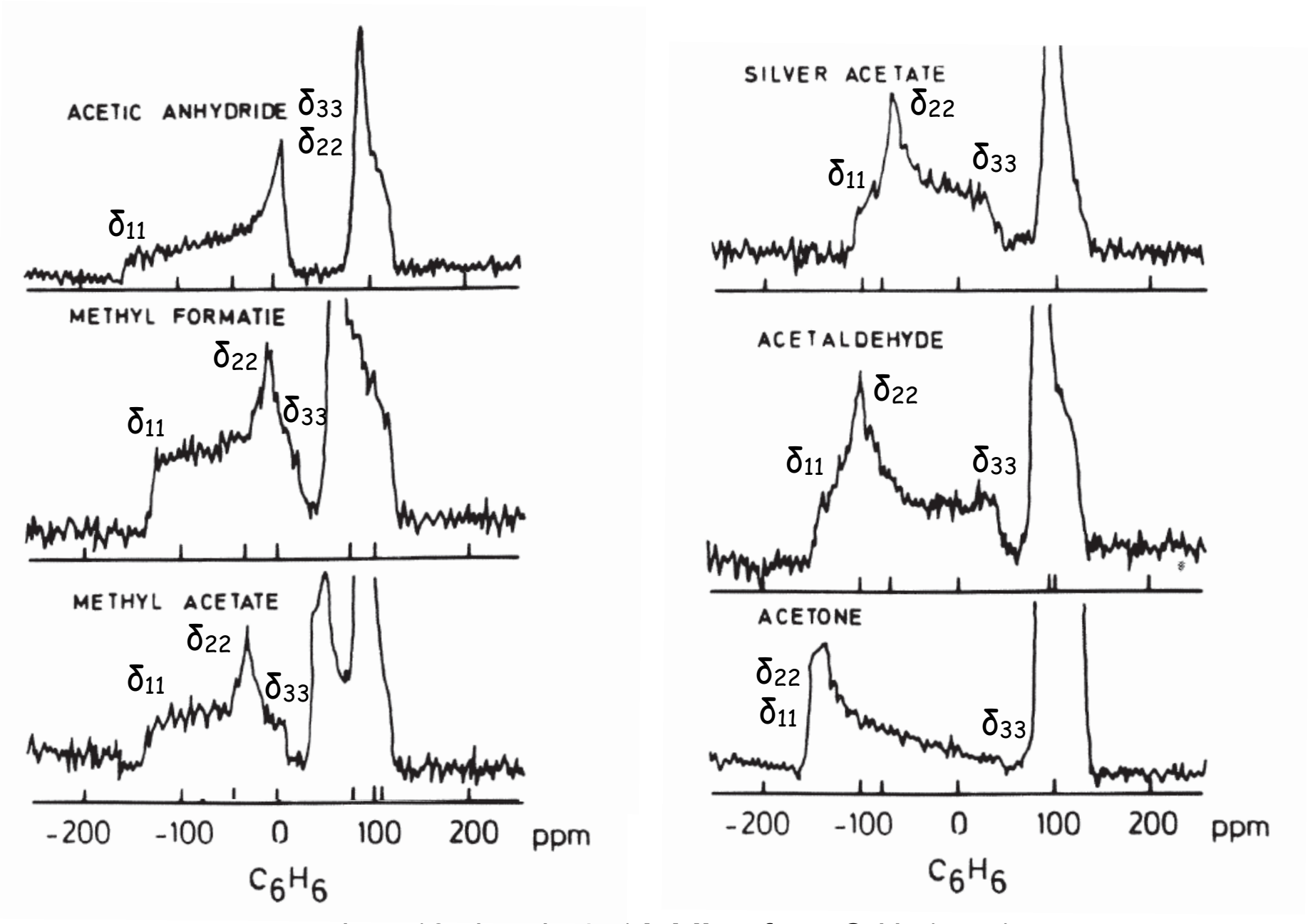


highly symmetric environment shielding is very similar in all directions very small CSA

asymmetric environment shielding is quite different in all three directions large CSA, large asymmetry parameter

axially symmetric environment shielding is quite different in two directions (⊥ and ∥ to the molecular axis) large CSA, no asymmetry

## Chemical Shift Anisotropy

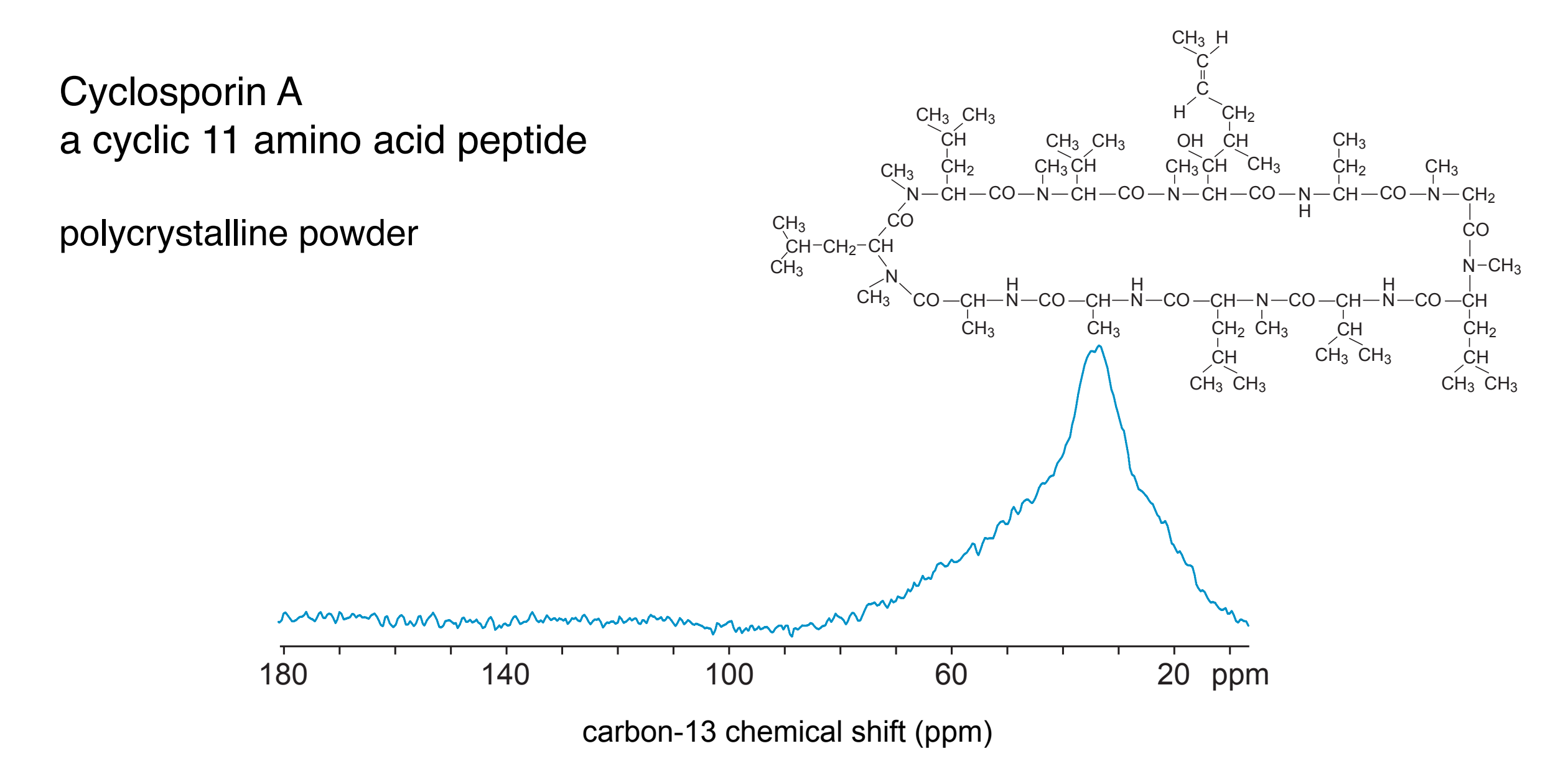


carbon-13 chemical **shielding** from C<sub>6</sub>H<sub>6</sub> (ppm)

Chemical shift anisotropy is a sensitive reporter of electronic structure.

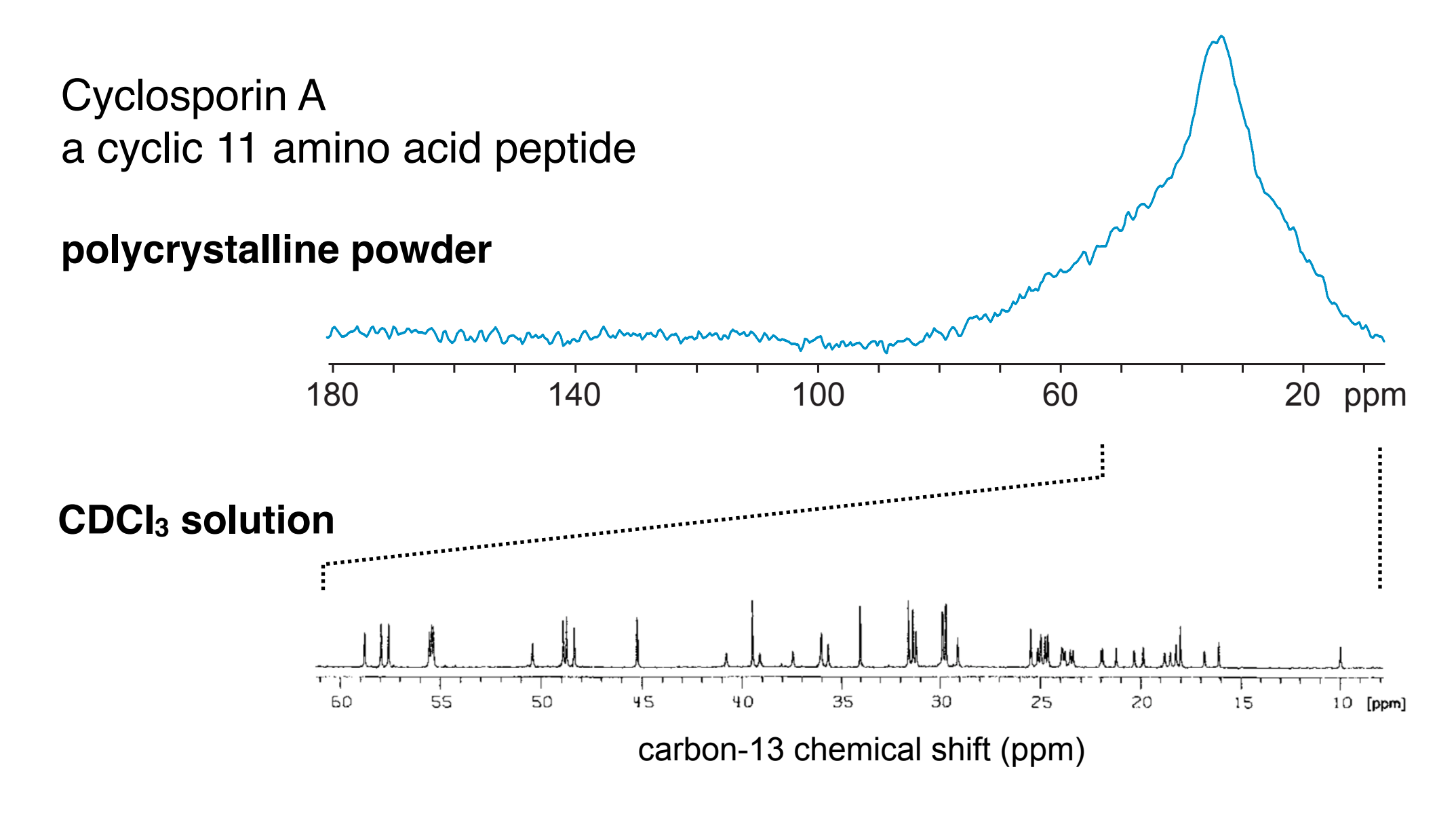
homework: work out the chemical basis for the difference in CSA between acetic anhydride and acetone

# Powder Spectra Have Low Resolution



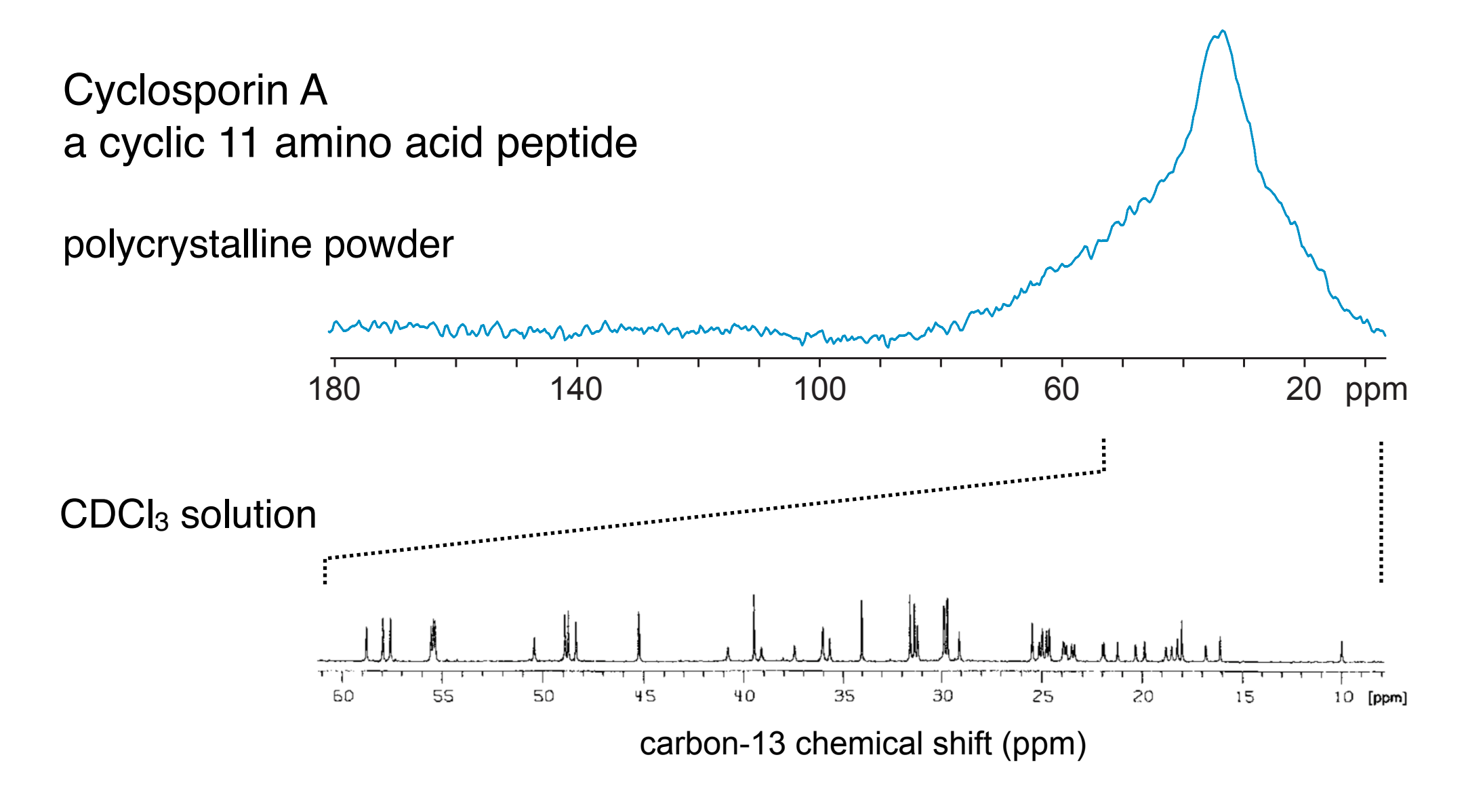
In molecules with many different nuclei, powder spectra will overlap, and resolution is lost. Many overlapping powder patterns make spectra unreadable. No access to pertinent chemical information.

# How can we regain high-resolution?



One simple way to gain resolution is by dissolving the sample in a liquid. Why?

# How can we regain high-resolution?



Rotational molecular motion (usually referred to as rotational diffusion) with a correlation time  $\tau_c$  much faster than  $1/\Omega$  will result in a spectrum in which only the average value of the chemical shift is observed. (Think of it as rapid exchange between all orientations.) For each type of nucleus, it will be the same for all the molecules in the sample:  $\delta_{iso}$ .

Idea: Impose motions on the sample, which will average the anisotropic component to zero. Do these motions have to be low symmetry? (SO(3)?)

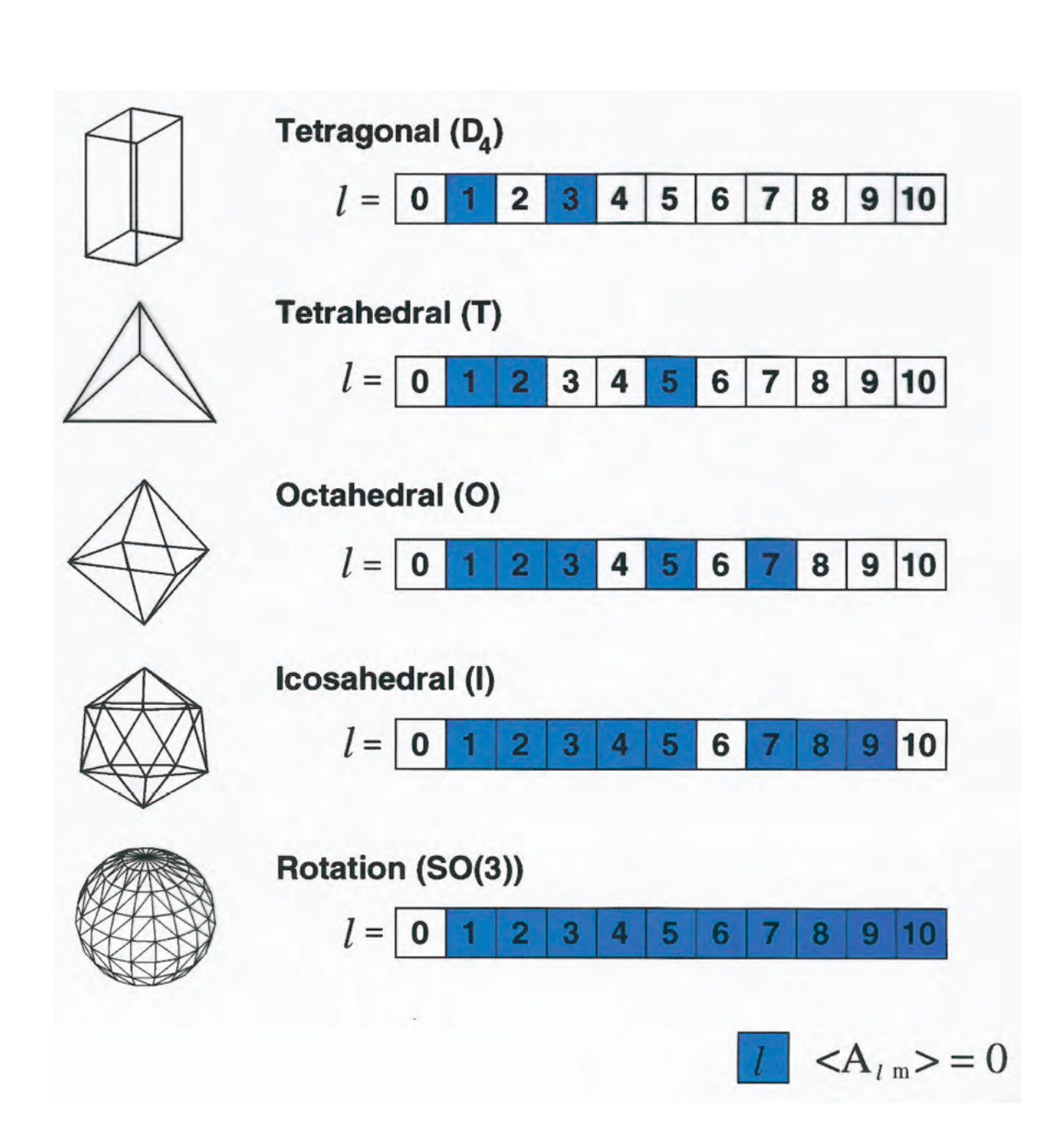
# **Coherent Averaging**

What is the simplest motion that will remove the anisotropic part of the interaction? Does it have to be random isotropic rotational motion?

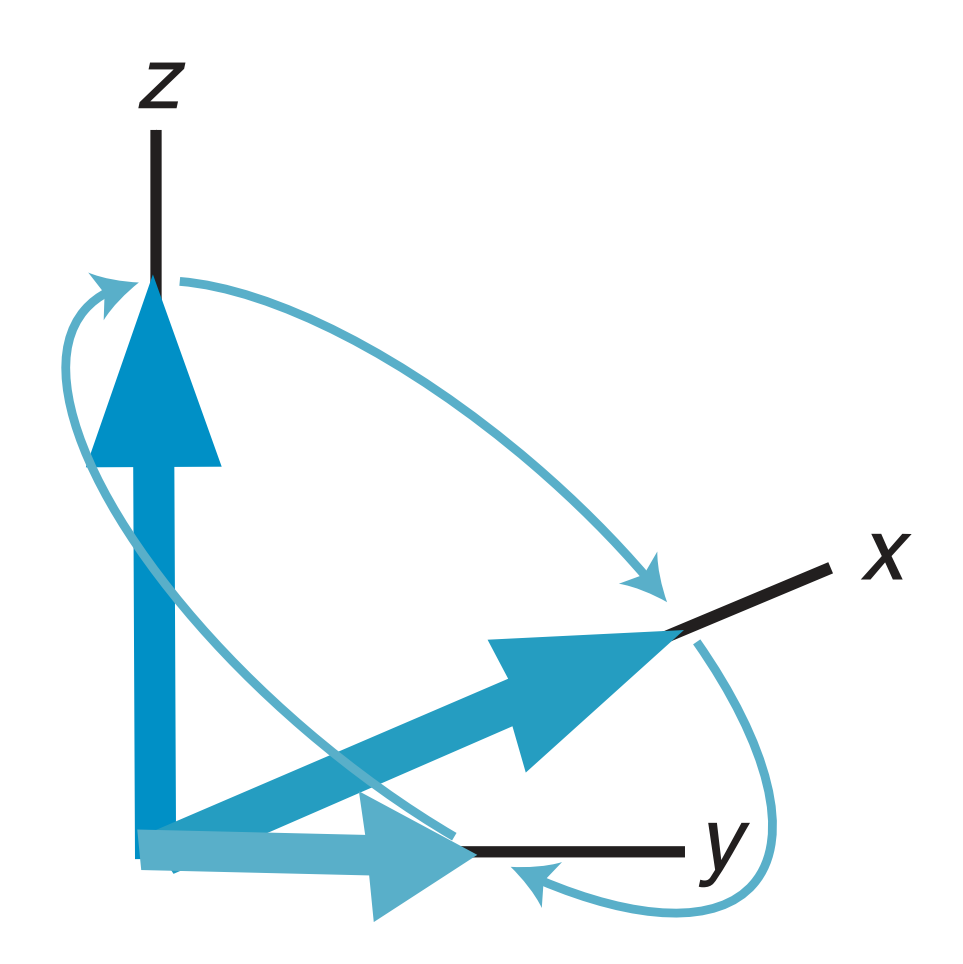
By comparing the symmetry of the interaction (here 2nd rank spherical harmonics) and the symmetry of a given motion, we can determine to what extent that motion will average the interaction. Group theory gives us the answer.

We find that motions with tetrahedral or octahedral symmetry are already sufficient to average interactions with a 2nd rank spatial dependence to zero.

For example, a motion with octahedral symmetry consists in jumping between the three orientations that point along the x, y and z axes of a cube.



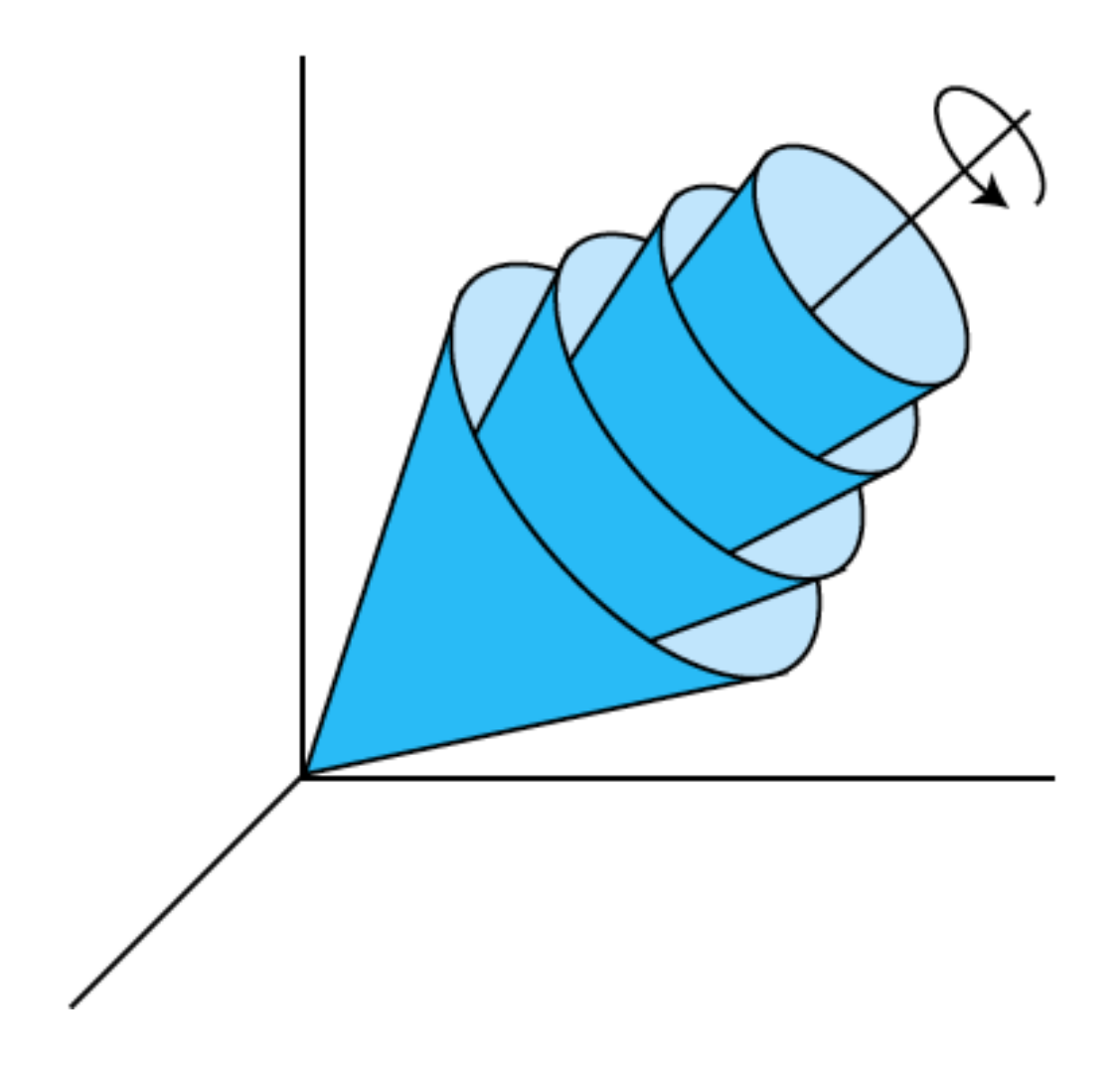
## Coherent Averaging: Magic Angle Hopping



A motion with octahedral symmetry consists in the sample **jumping** between the three orientations that point along the x, y and z axes of a cube.

This can also be achieved by **spinning** the sample around the body diagonal of the cube (the 1,1,1 axis)

# Coherent Averaging: Magic Angle Spinning



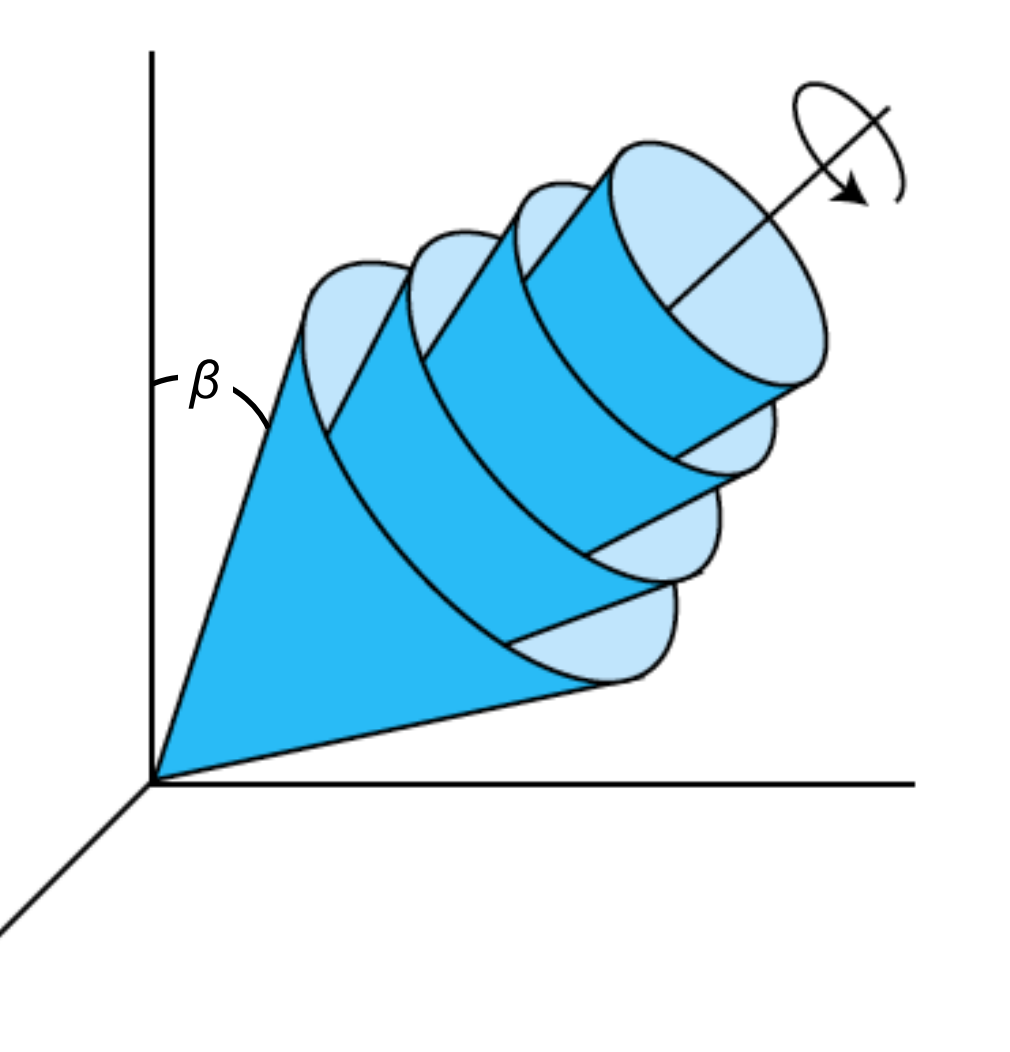
Another way to visualise this is to consider that physically spinning the sample produces an **average orientation** that is aligned with the spinning axes, for any given initial orientation of the interaction.

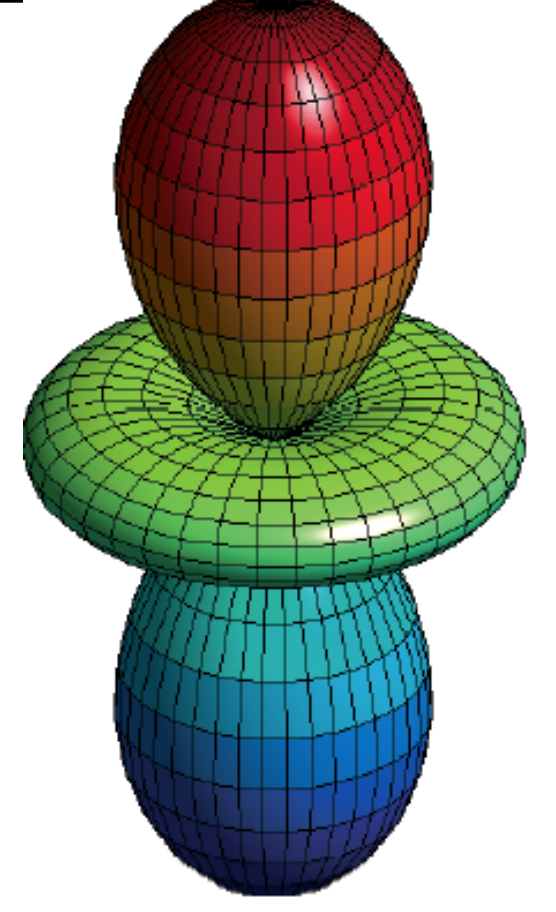
# Coherent Averaging: Magic Angle Spinning

For an axially symmetric tensor (i.e. either with  $\delta_{22} = \delta_{33} = \delta_{xx}$  and  $\delta_{11} = \delta_{11} = \delta_{22} = \delta_{xx}$  and  $\delta_{33} = \delta_{zz}$ ) the chemical shift is given by:

$$\delta = \delta_{iso} + (\delta_{zz} - \delta_{iso}) \left( \frac{3cos^2\beta - 1}{2} \right)$$

where  $\beta$  is the angle between the  $\delta_{zz}$  axis and the magnetic field.





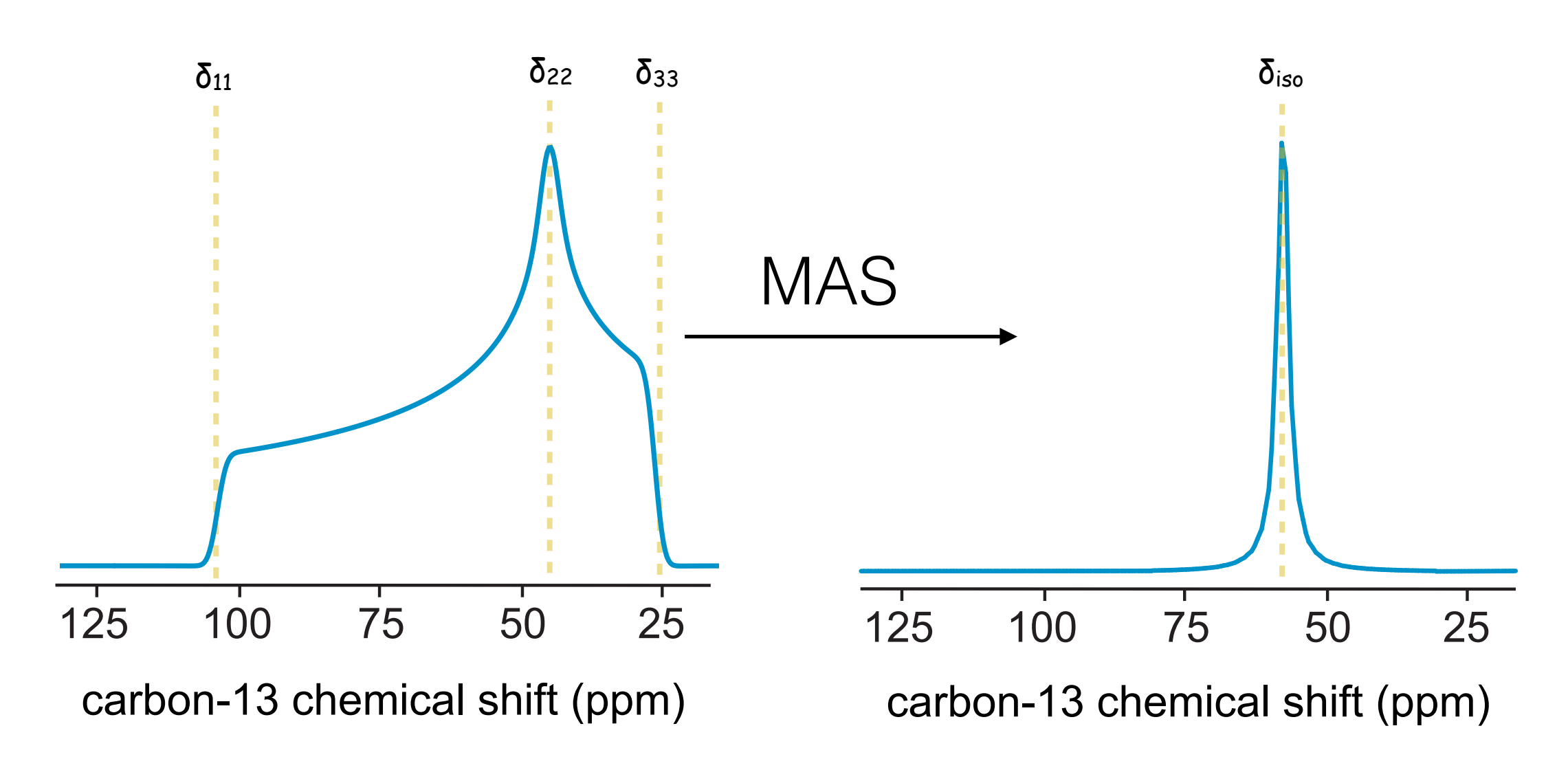
Spinning the sample makes all crystallites appear to have an average  $\beta$  angle  $\langle \beta \rangle$  that is oriented along the spinning axis.

If the axis of spinning is 54.7°, then  $\langle \beta \rangle$  = 54.7° and  $3\cos^2 \langle \beta \rangle$  - 1 = 0so that  $\langle \delta \rangle = \delta_{iso}$ 

## Magic Angle Spinning

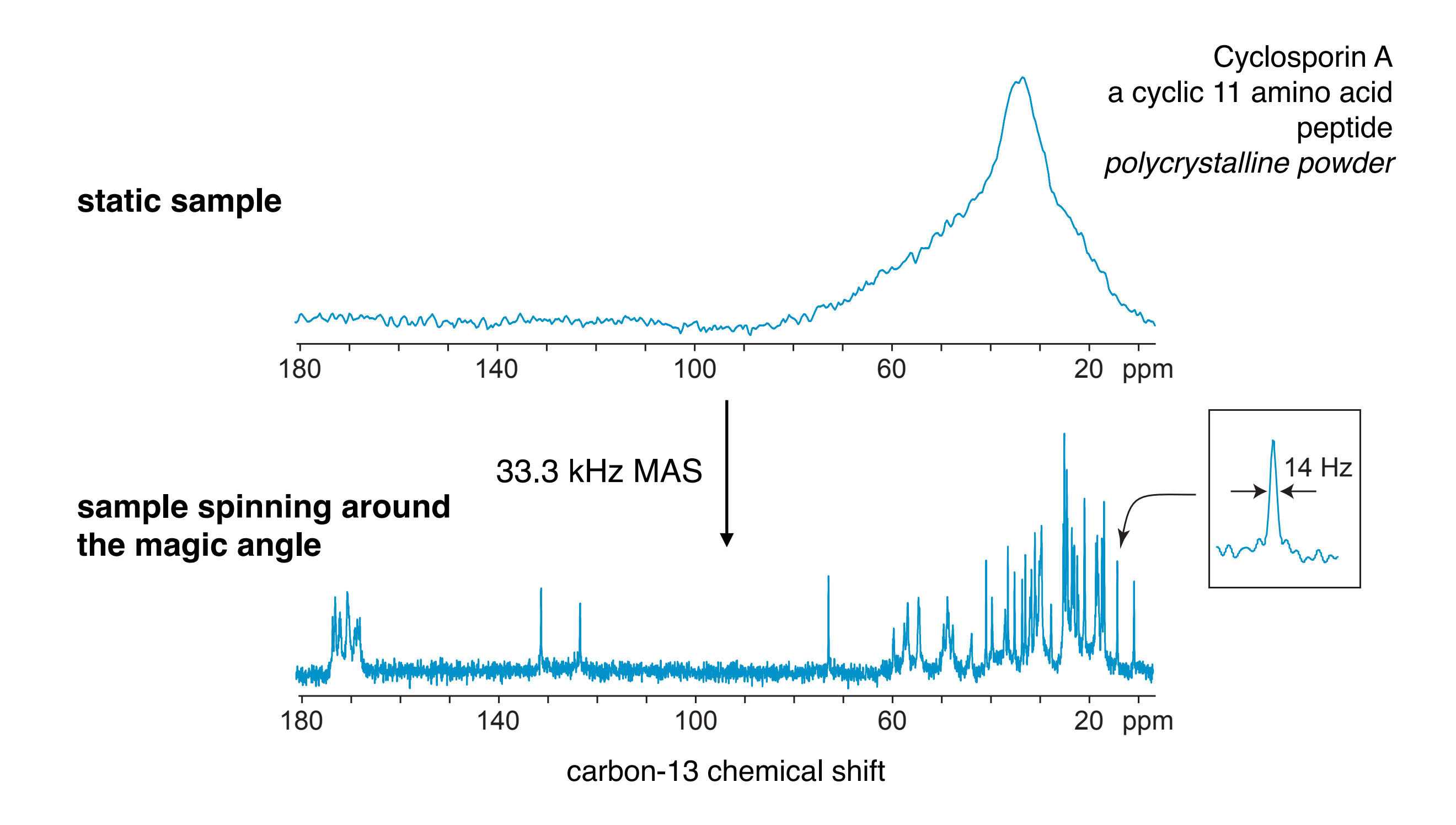
If the angle of the spinning axes is set to 54.7° wrt to B<sub>0</sub>, then all orientations will have the same average frequency.

It is the center of gravity of the powder pattern: the isotropic chemical shift



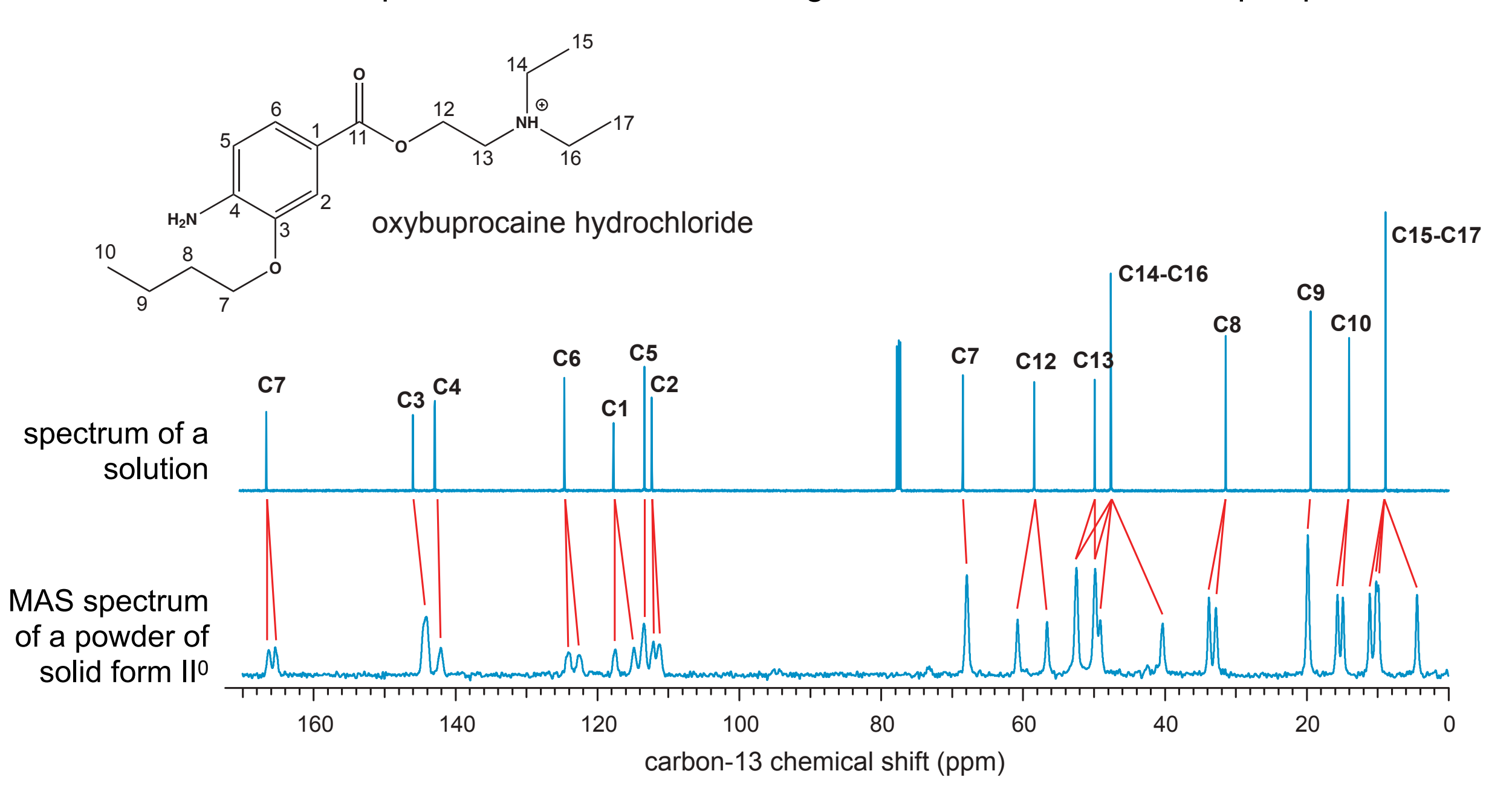
$$\delta_{iso} = (\delta_{11} + \delta_{22} + \delta_{33})/3$$

# Magic Angle Spinning



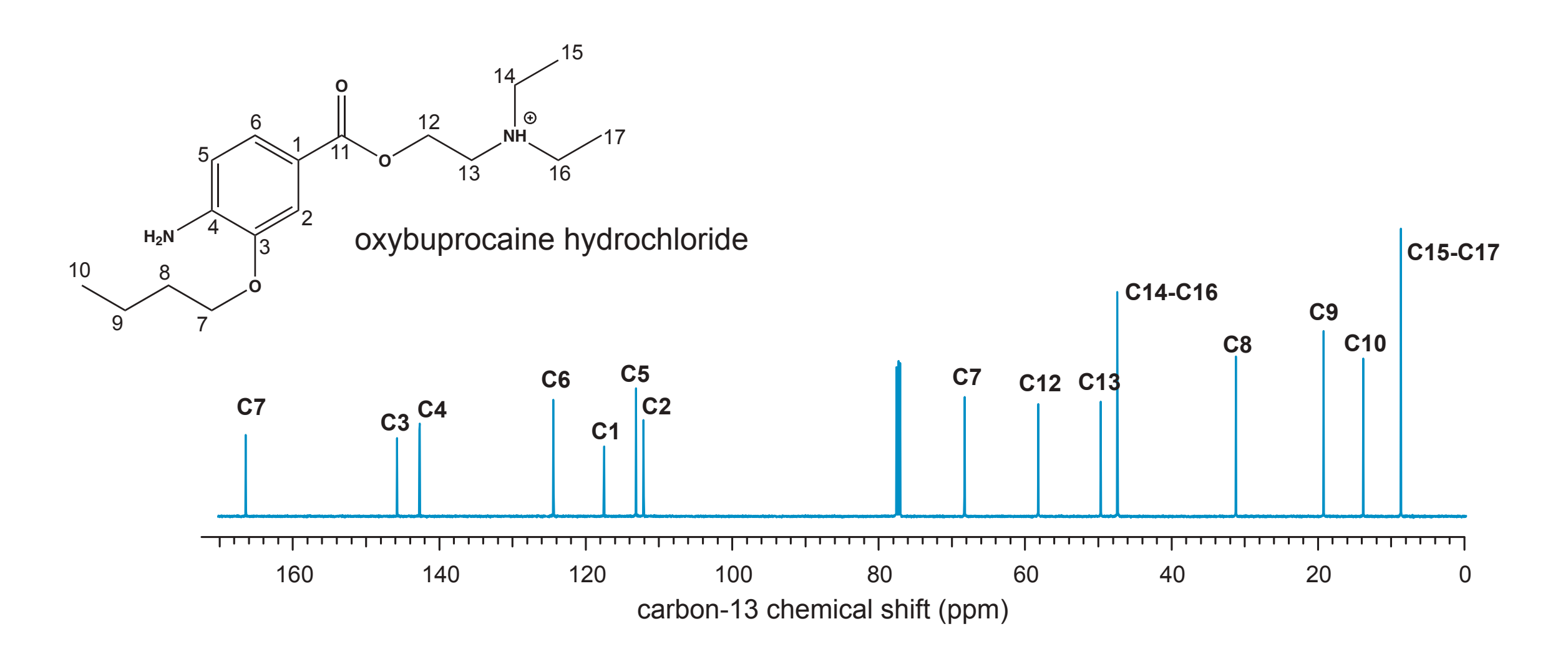
# Magic Angle Spinning

Note that the isotropic chemical shift can change between the solid and liquid phases



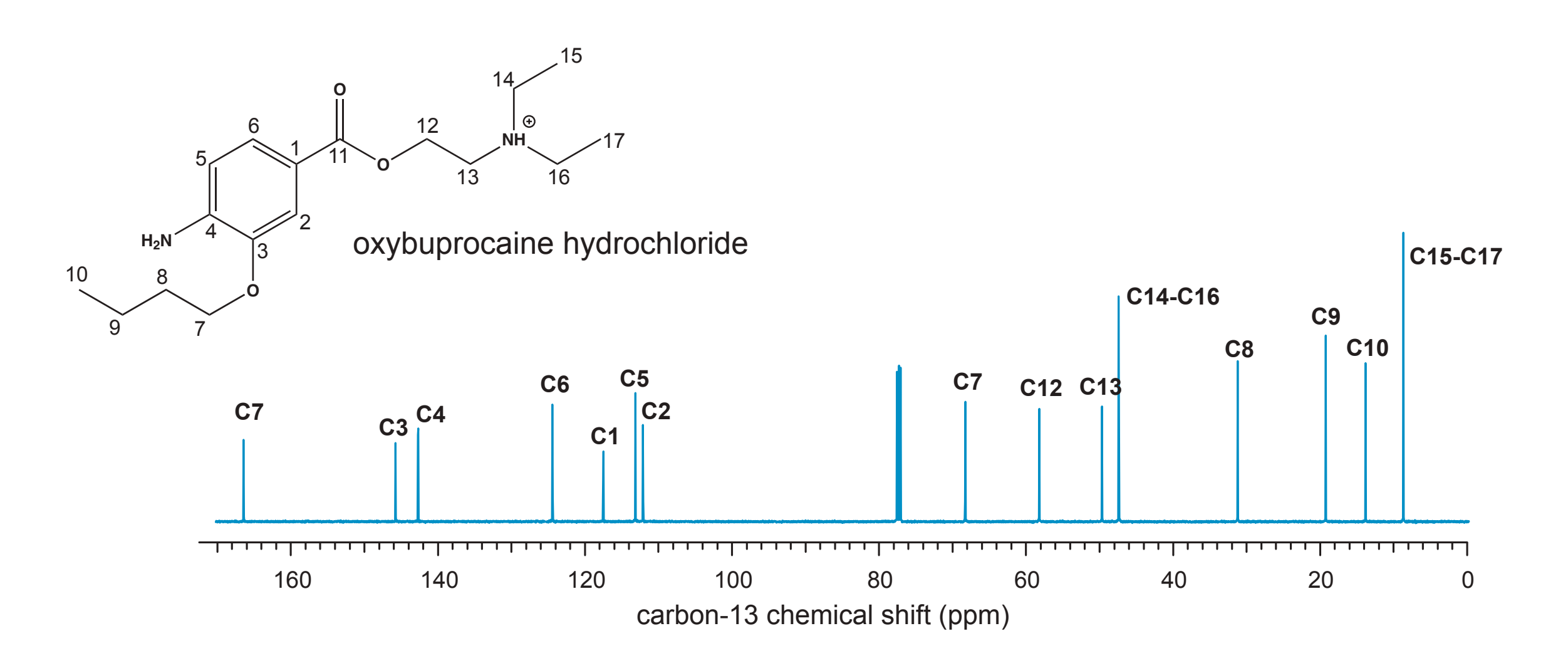
Chemical shifts are exquisite reporters of chemical structure and dynamics

# Coherent Averaging II: Take a closer look at solution-state carbon-13 spectra



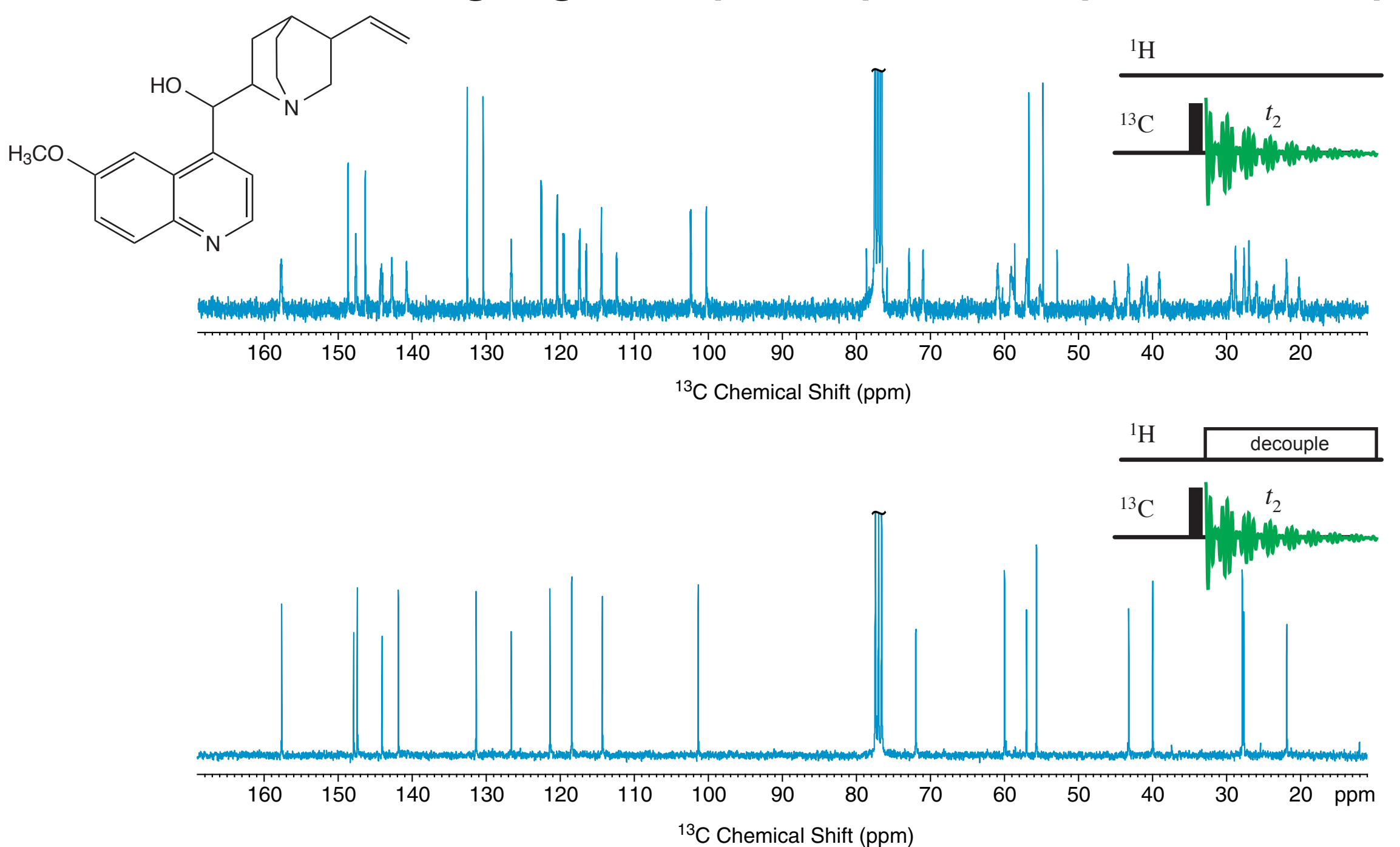
What is the fine structure of the peaks? Why?

# Coherent Averaging II: Take a closer look at solution-state carbon-13 spectra



How could we remove the heteronuclear J couplings?

# Coherent Averaging in Spin Space: Spin Decoupling



By applying a train of  $\pi$  pulses to the heteronucleus (usually  $^1H$ ), or by continuous irradiation of the heteronucleus, we can average the heteronucleur J coupling to zero. The decoupled spectrum has better resolution & sensitivity. Carbon-13 NMR spectra are

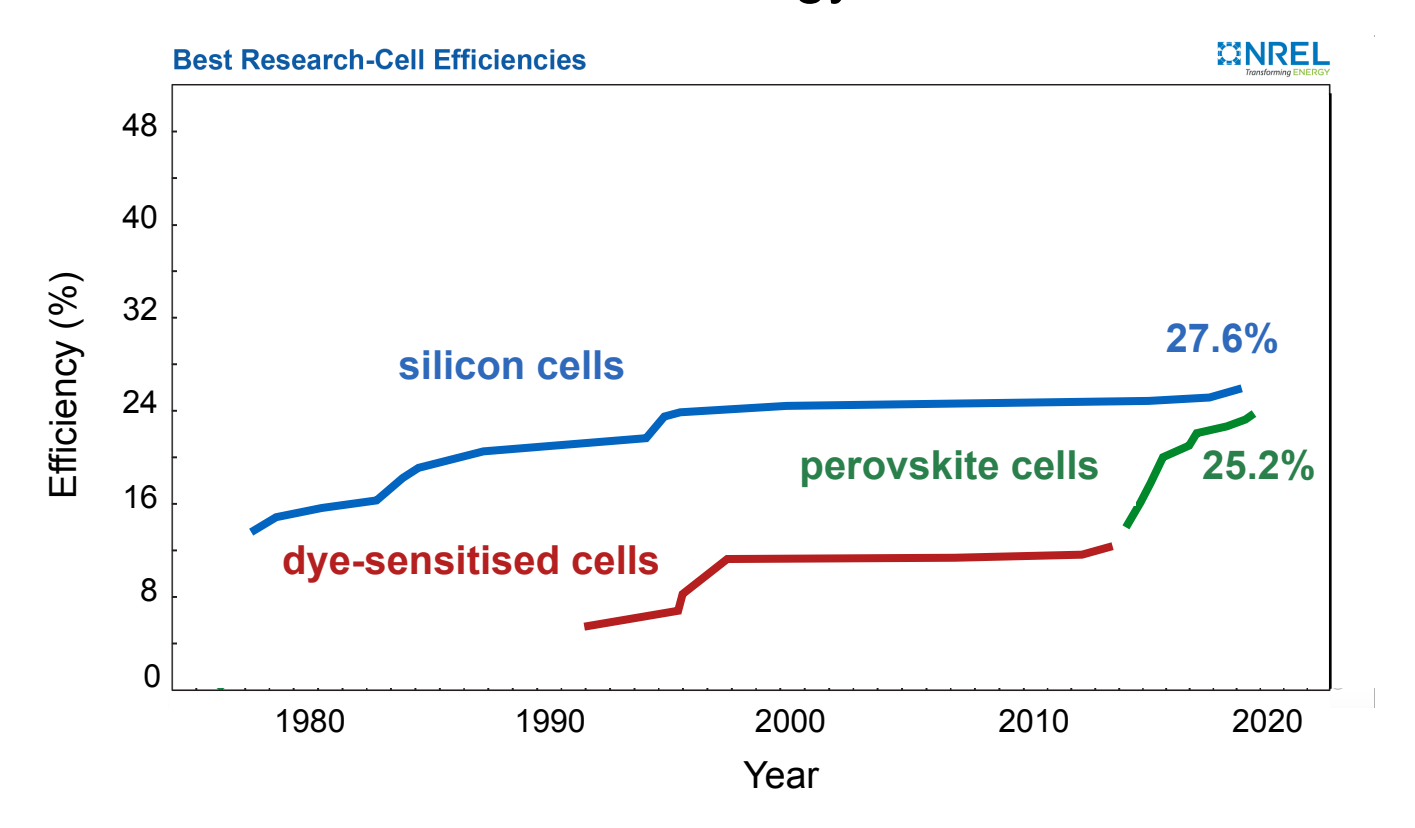
almost always recorded with decoupling.

# Conclusions

- The chemical shift is anisotropic. The NMR frequency depends on the orientation of the molecule with respect to the magnetic field.
- Anisotropic interactions are described by a tensor. The CSA tensor is second rank, and has three principle values in an axes system described by three angles with respect to a reference frame fixed in the molecule.
- The full CSA tensor can be determined from NMR of single crystals.
- Powder spectra are the sum of spectra from all orientations. Line shapes are characteristic of the tensor principle values.
- By rapidly spinning the sample around an axes at an angle of 54.7° with respect to the main field, the anisotropy can be averaged to the isotropic value for any crystallite orientation. We refer to this as coherent averaging. Magic angle spinning yields a high-resolution isotropic spectrum from a powder.
- Coherent averaging can also be applied in spin space. By irradiating protons during acquisition of carbon-13, heteronuclear scalar couplings can be averaged to zero (decoupled).

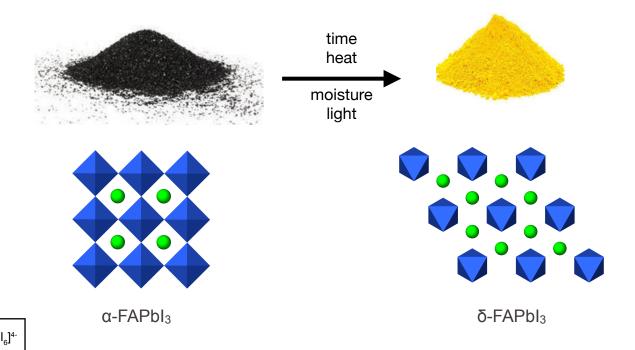


# Perovskite-based cells: the fastest-advancing solar technology to date





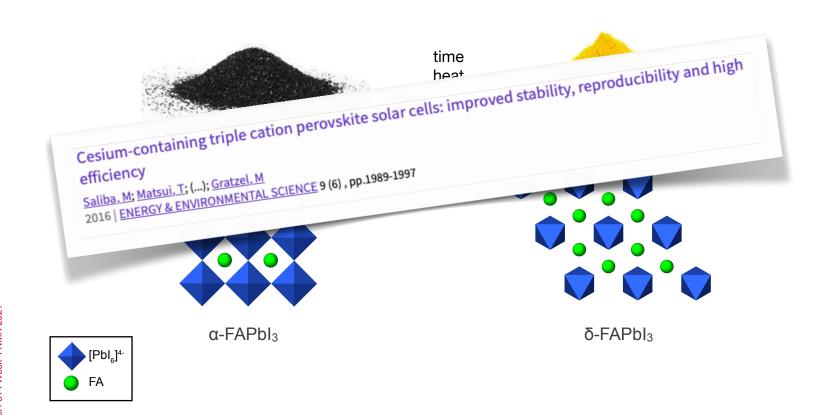
#### Degradation of α-FAPbI<sub>3</sub> under environmental conditions



FΑ

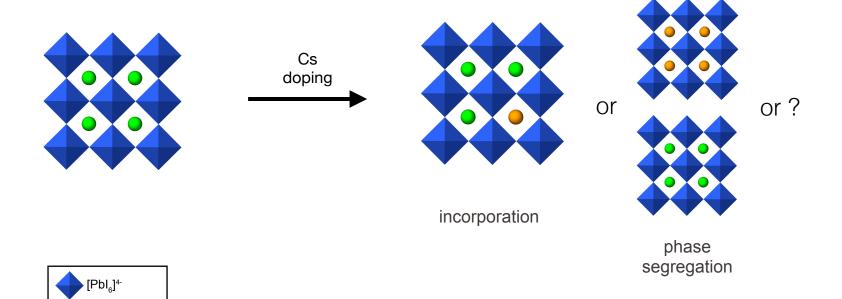


### Degradation of $\alpha\text{-FAPbI}_3$ under environmental conditions





#### Atomic-level mechanism of molecular modulators

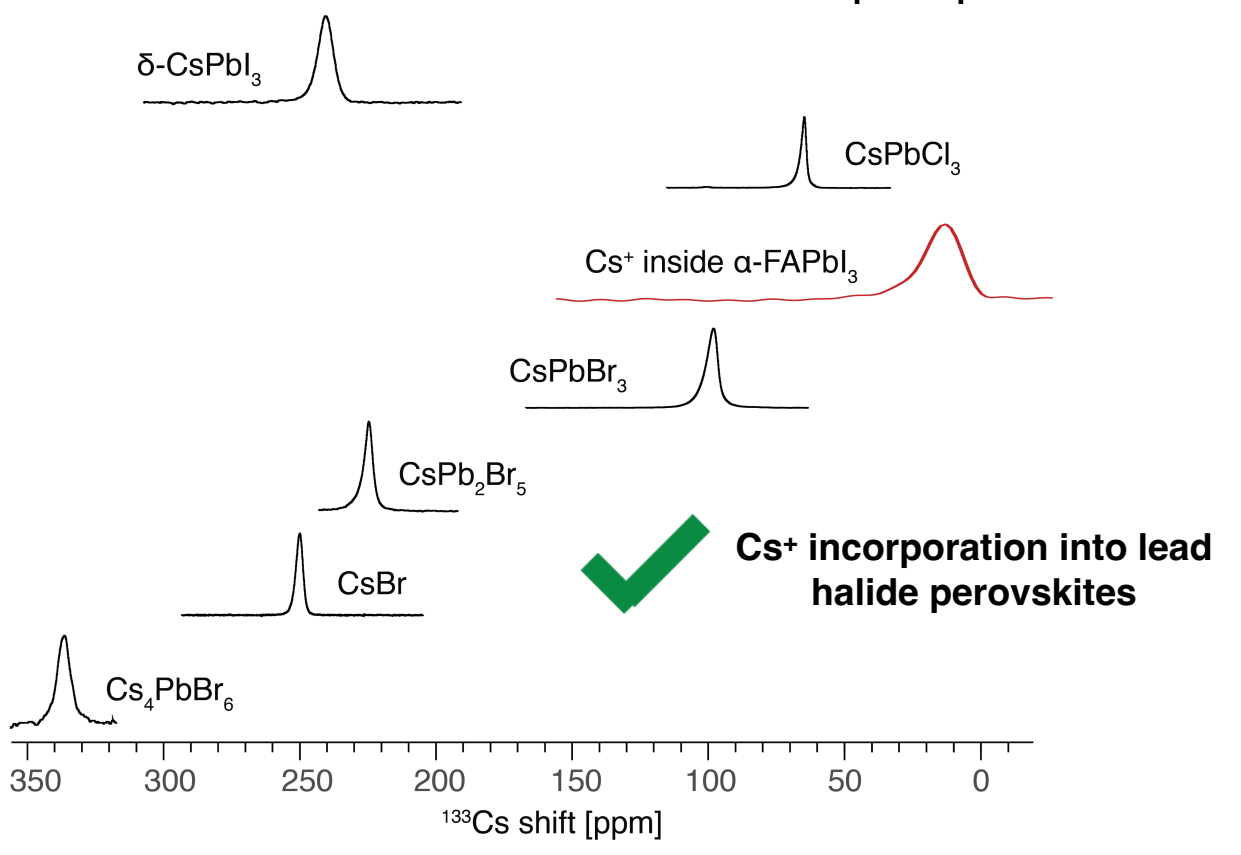


FΑ

MA/Cs/Rb/K



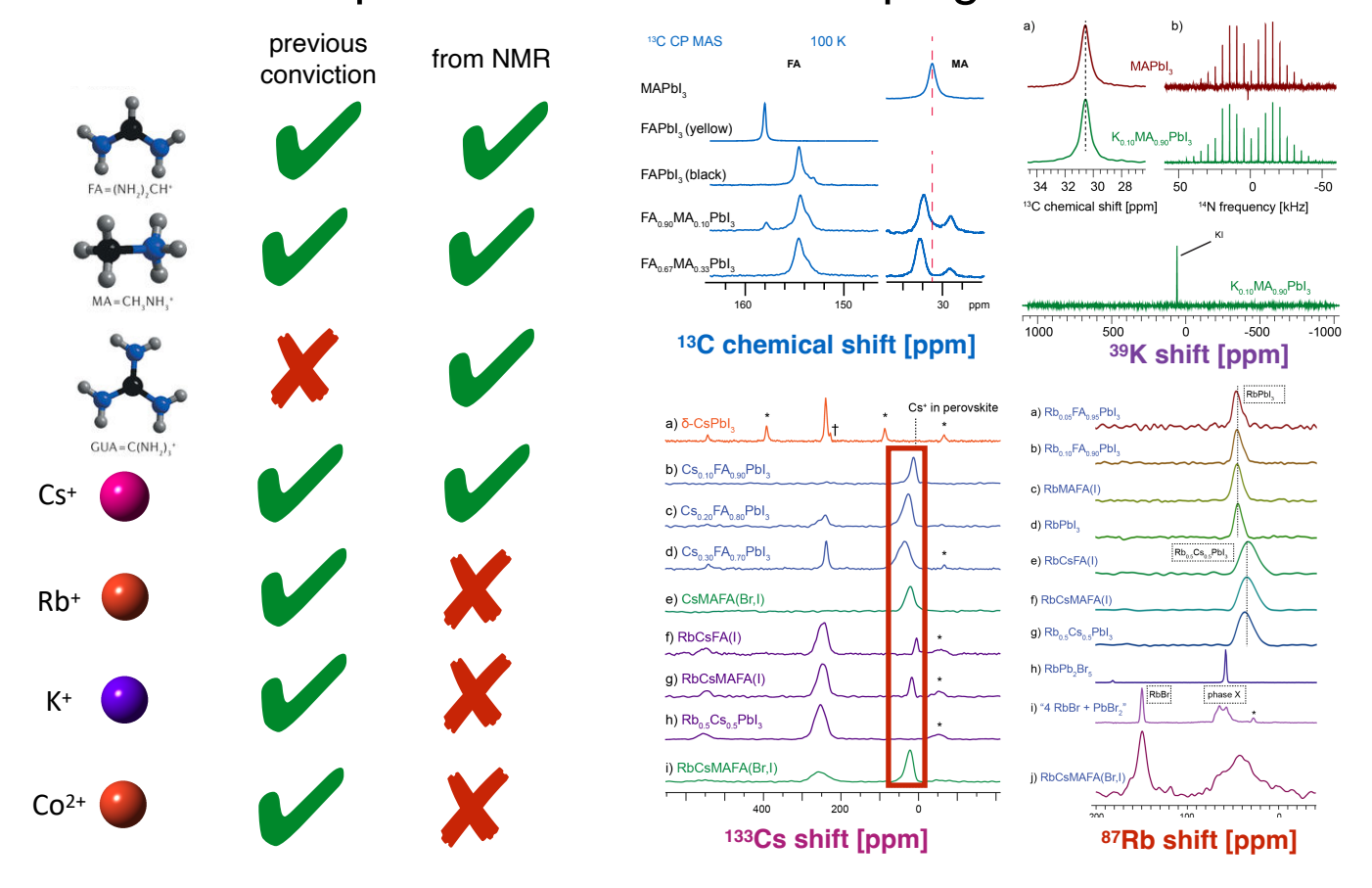
#### <sup>133</sup>Cs solid-state MAS NMR of cesium-doped perovskites



■ CH-314 Week 4 NMR 2021



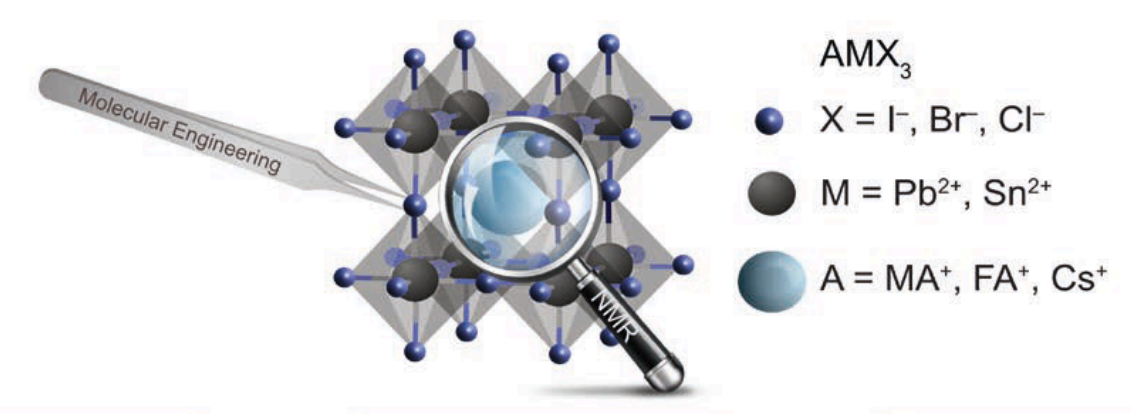
#### Phase Composition and Cation Doping in Perovskites

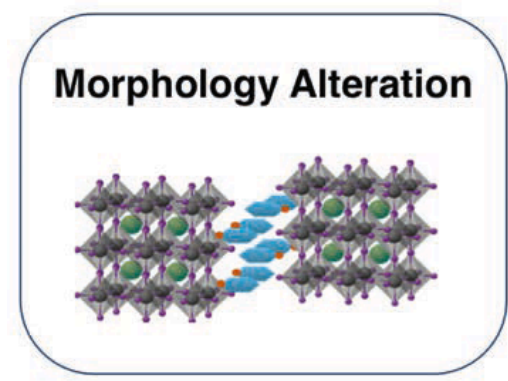


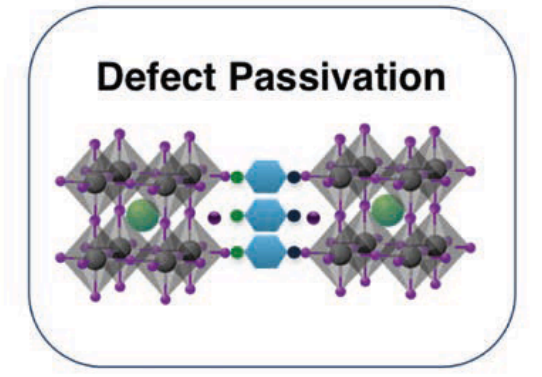
CH-314 Week 4 NMR 2021

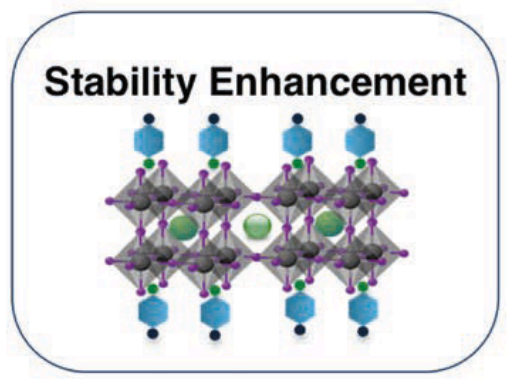


# NMR determination of the atomic-level mechanism of modulators leads to a paradigm shift in design principles



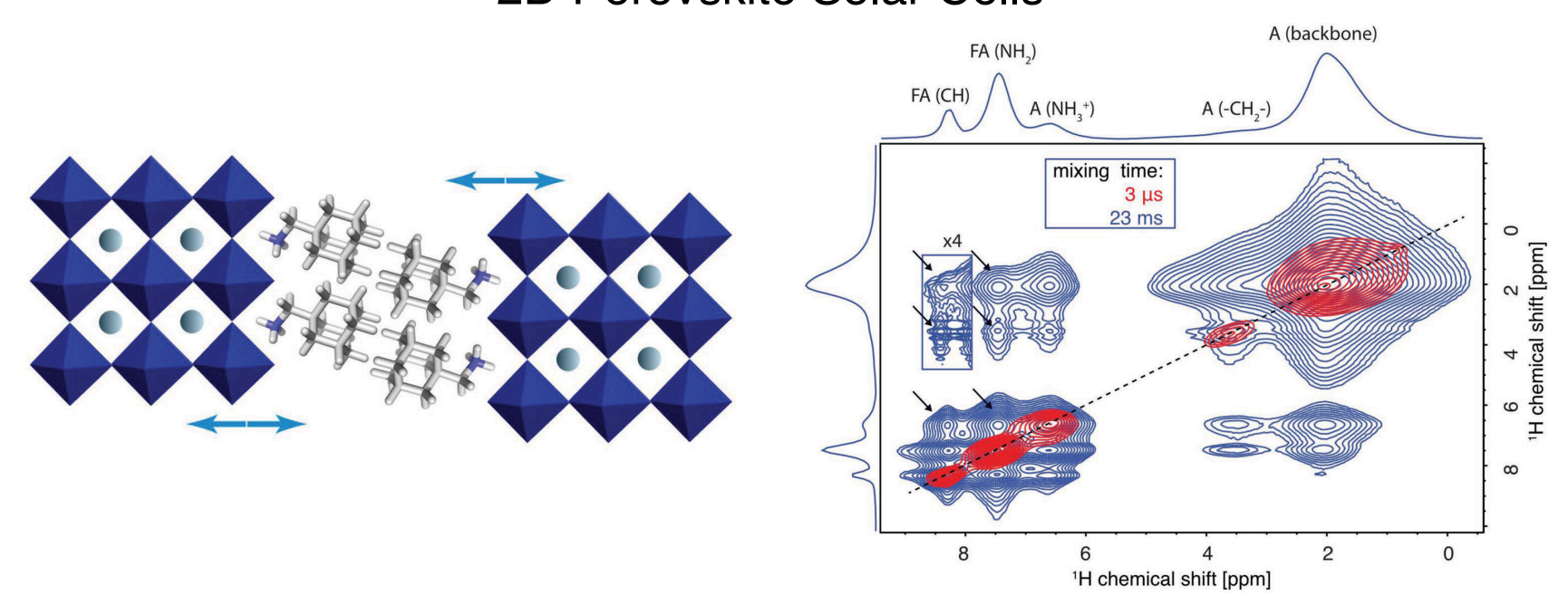








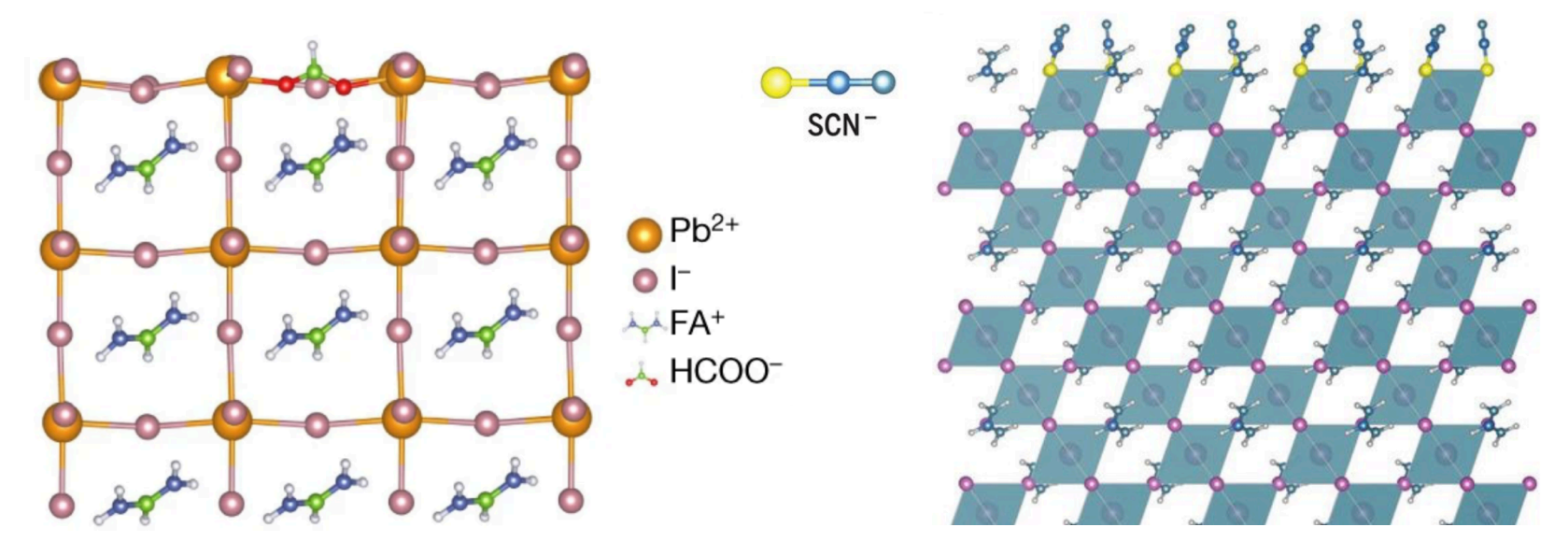
# Supramolecular Engineering of FA-Based Layered 2D Perovskite Solar Cells



Direct observation of the formation of the 2D layered Ruddlesden-Popper (RP) phase



# Atomic-Level Insights for NMR Lead to New Design Strategies that Yield New Record Holding Materials for Efficiency and Stability

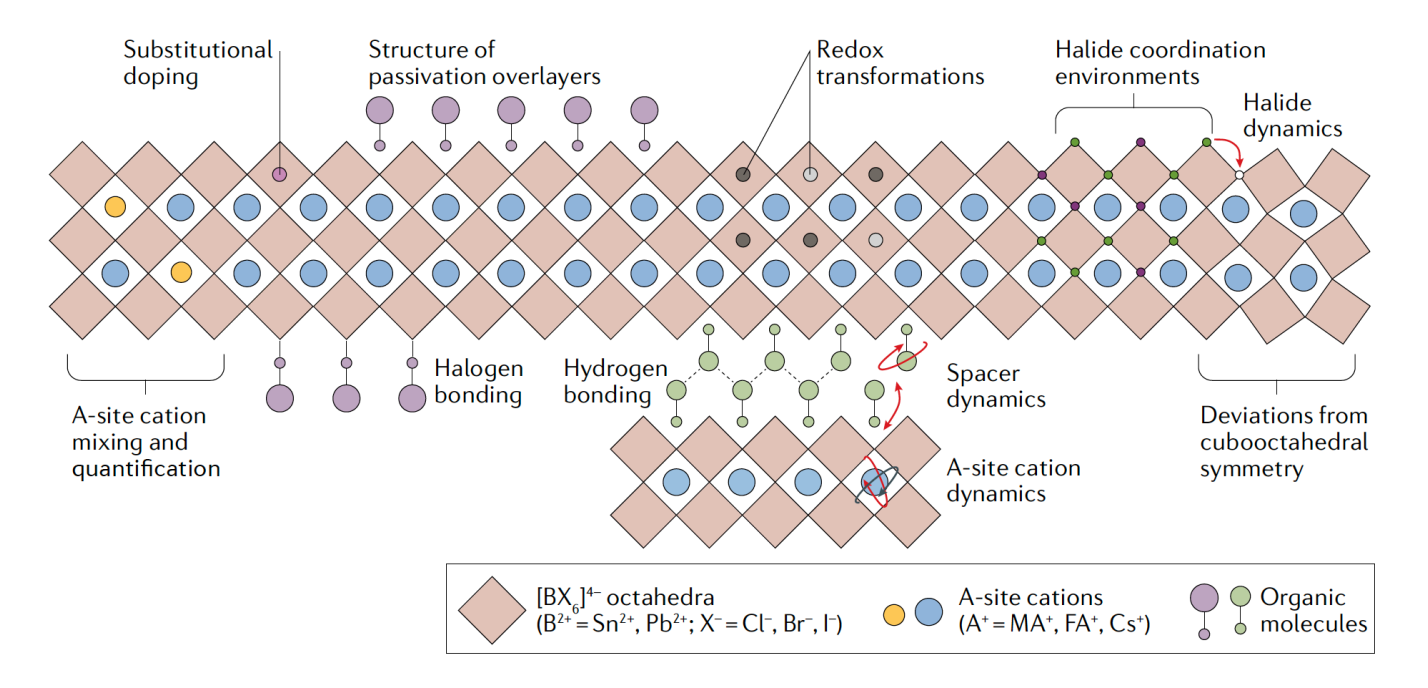


Jeong, *et al.*, "Pseudo-halide anion engineering for  $\alpha$ -FAPbI(3) perovskite solar cells," *Nature*, (2021).

Lu et al., "Vapor-assisted deposition of highly efficient, stable black-phase FAPbI(3) perovskite solar cells," *Science* **370**, 74 (2020).



# NMR spectroscopy probes multiple aspects of microstructure, dynamics and doping of metal halide perovskites



CH-314 Week 4 NMR 2021

Kubicki, Stranks, Grey, Emsley, *Nat. Rev. Chem.* **5**, 624 (2021). https://doi.org/10.1038/s41570-021-00309-x

# Objectives

- Learn to read research articles
- Learn how to apply NMR to real-world problems

# Case Studies

### For each of the papers:

- What is the subject of the research & why is it interesting or important?
- What is the precise objective of this study?
- What is/are the approach(es) used?
- What role does NMR play?
- What are the conclusions? How do the NMR results support the conclusions?

# Case Study 1

### Drug Discovery by NMR

# Discovering High-Affinity Ligands for Proteins: SAR by NMR

Suzanne B. Shuker, Philip J. Hajduk, Robert P. Meadows, Stephen W. Fesik\*

# Homework

For next week, in the same groups as for the problem classes, choose one paper for each group from the papers on Moodle.

Prepare a short (**10 min**) **joint** (i.e. every member should say at least one thing) presentation to the class for next week's course in which you present and analyse the paper addressing the 5 terms we have used this week.

Each presentation will be followed by a group discussion.